

MASTER

Validating a 3D-printed structure optimised via topology optimisation

"Does a 3D-printed optimised beam have the same structural properties as an optimisation tool prescribed?"

van Rijssen, Bram

Award date:
2023

[Link to publication](#)

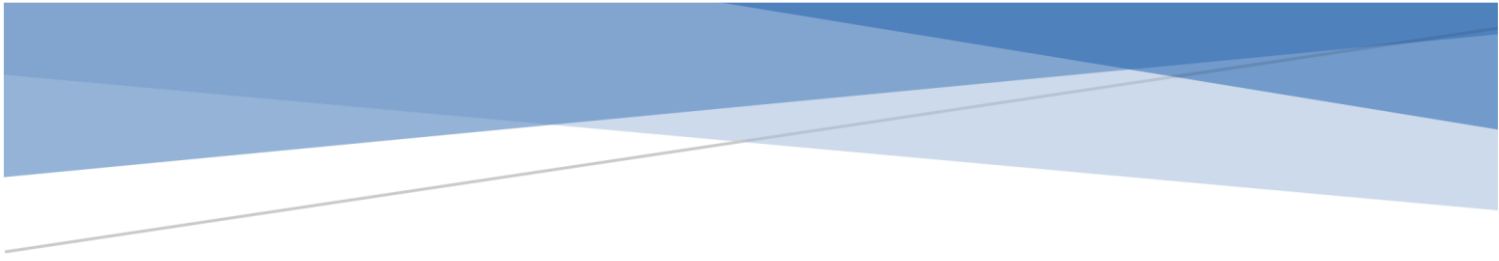
Disclaimer

This document contains a student thesis (bachelor's or master's), as authored by a student at Eindhoven University of Technology. Student theses are made available in the TU/e repository upon obtaining the required degree. The grade received is not published on the document as presented in the repository. The required complexity or quality of research of student theses may vary by program, and the required minimum study period may vary in duration.

General rights

Copyright and moral rights for the publications made accessible in the public portal are retained by the authors and/or other copyright owners and it is a condition of accessing publications that users recognise and abide by the legal requirements associated with these rights.

- Users may download and print one copy of any publication from the public portal for the purpose of private study or research.
- You may not further distribute the material or use it for any profit-making activity or commercial gain



VALIDATING A 3D-PRINTED STRUCTURE OPTIMISED VIA TOPOLOGY OPTIMISATION

“Does a 3D-printed optimised beam have the same structural properties as an optimisation tool prescribed?”

Title Validating a 3d-printed structure optimised via Topology optimistaion
Subtitle Does a 3D-printed optimised beam have the same structural properties
as an optimisation tool prescribed?

Date 30/06/2023
Version 1.2 (Final)
Place Eindhoven

Author B. (Bram) van Rijssen
Student number 1319469
Email address b.vanrijsseen@student.tue.nl
bram.vanrijsseen@live.nl

Graduation committee prof. dr. ir. T.A.M. (Theo) Salet (Chairman)
dr. ir. R.J.M. (Rob) Wolfs
prof. dr. ir. P.H.W. Habraken

PREFACE

This research is set up as a graduating project for the completion of the master program in Structural Engineering and Design at the Architecture, Building and Planning academy at the Eindhoven University of Technology. The research topic is a follow-up on the graduation project of Jelle Versteeg: 'An integrated approach for topology optimization and print path generation of cable-reinforced 3D printed concrete structures'.

This project has been carried out under the supervision of Prof. Dr. Ir. T.A.M. (Theo) Salat and Dr. Ir. R.J.M. (Rob) Wolfs. I would like to thank my supervisors for their excellent guidance and innovative meetings.

Additional, I want to thank my fellow students for helping and supporting me during this process. In special, I want to thank Matthew Ferguson, Jelle Versteeg and the supervisors at the structural lab for helping me in the printing process.

Bram van Rijssen

Tilburg, April 2023

ABSTRACT

Optimisation tools and 3D concrete printing together combines the strength of placing material only where it is needed, without the use of formwork. Previous studies have developed tools to optimise structures and transform them into printable structures. On paper, these structures perform as expected, but it is uncertain if the printed structures behave the same as the optimised structures. That is why this research is set up to validate the optimisation tools. The research is divided into three different stages; optimisation, printing and testing.

The optimisation starts with a set of material properties and boundary conditions that represents the concrete and test setup used. A topology optimisation script optimises the structures, prescribing material at locations where it is needed and leaving empty spaces where the material doesn't contribute to the strength and stiffness of the structure. The next script, the toolpath generator, transforms the optimisation output into a 2D printing route. Finally, a grasshopper script transforms the 2D printing route into a set of 3D coordinates for robot control.

The 3D concrete printing process exists out of several detached elements. The concrete is mixed by hand and poured into a small concrete pump which pumps it through a hose out of a nozzle. The nozzle is attached to a small ABB robot. A continuous flow of concrete, combined with the movement of the robot, creates the printing process.

The research conducted two different case studies. The first optimised structure is a 600x100mm simply supported beam, loaded with a point load in the middle. The second case study has the same settings but with an increased height, making it a 600x200mm beam. Two different versions are made for the second case study, trying to improve the execution. Benchmark beams are made for both case studies for comparison. These benchmark beams consist of solid, casted concrete with the same dimensions.

A total of 26 structures (Benchmark beams and printed structures combined) are tested via a 3-point bending test. Test samples are made for every set of beams, giving insight into the material properties of the concrete on the day of testing. Comparisons in data are drawn on four different levels, namely, comparing results within series, comparing results between series, comparing prescribed weight vs measured weight and experimental results are compared to the numerical results.

After comparing, analysing and debating the results, the following end verdict is drawn up; The system's performance of the printed structures excels the performance of the benchmark beam in terms of kN/kg ratio. The printed structure fails to achieve the expected stiffness. Reasons for the deviating results are attributable to the execution process. In terms of weight, the printed structure represents the prescribed structure from the optimisation process.

The overall conclusion in the validation process is that the printed structure comes close to representing the prescribed structure but isn't there yet. This has mainly to do with the difference in stiffness. Further optimisation of the printing process should bring these properties closer to the optimisation output.

TABLE OF CONTENT

Preface	4
Abstract.....	5
1. Introduction.....	7
1.1. Topology-optimized 3d structures	7
1.2. The challenge	8
1.3. Research questing	9
1.4. Thesis outline	10
2. Software explanation	11
2.1. Topology optimisation (Python).....	11
2.2. Print path	12
2.3. Rapid code (Grasshopper).....	14
2.4. Karamba (Grasshopper)	19
3. Methodology	20
3.1. Printing.....	20
3.2. Testing.....	23
3.3. Test samples.....	24
4. Case study.....	25
4.1. Topology optimisation input.....	25
4.2. Case 1	26
4.3. Case 2	32
5. Results	36
5.1. Result.....	36
6. Comparison and discussion	40
7. Conclusion and Recommendation.....	58
7.1. Conclusion	58
7.2. Recommendation.....	60
References	61
Appendix.....	62

1. INTRODUCTION

The demand for a more sustainable construction industry [1] is increasing, and different aspects of the industry are addressed to develop. In recent years the development of 3d printing has increased exponentially [2]. The advantages of high building efficient, low labour cost and less construction wastes compared to traditional construction technology makes it an technological interesting development. 3D printing technology has great potential on practical applications, such as affordable housing construction in low-income countries or complex constructions where the formwork is difficult in manufacturing.

The decline in materials combined with the pollution some products produces requires a material-efficient industry. This means, on the one hand, using materials that don't contribute to the pollution problem and, on the other hand, placing the materials only where it is needed. In other words, using the maximal potential of the material without over-capacitating. Sizing-, shape- and topology optimisation are all methods to obtain the maximal capacity with minimal material use. Sizing optimisation leads to an optimal relation between weight, stiffness, and dynamic behaviour. Shape optimisation tries to find the optimal shape by minimising a certain cost function while satisfying given constraints [3].

1.1. Topology-optimized 3d structures

Topology optimisation (TO) is a mathematical method that optimises material layout within a given design space for a given set of loads, boundary conditions, and constraints [4]. TO is different from sizing- and shape optimisation due to the freedom of shape it can attain within the given design space. Sizing- and shape optimisation is constrained to the predefined configurations.

The use of 3d technology combined with material optimisation grants a great opportunity. The 3d printer can place the material at any specific position without using formwork. Several studies have been conducted to develop a model method that can generate the optimal structure where material and performance are at their maximum potential. These models were designed and tested theoretically but have never been validated. Without such validation, there is no saying with certainty that the model represents the actual behaviour of the printed structure. Differences can be found in the failure behaviour, material behaviour, tension-compression zones, etc. All these aspects that can alter reality must be checked to validate the design model. This is where this research makes its start.



Figure 1 - 3d concrete printing

1.2. The challenge

The combination of 3DPC and an optimisation tool presents new challenges. Structures can be optimised with digital programs, tested digitally and confirmed digitally, but that doesn't mean it works perfectly in the real world. Traditionally, 3D-printed structures have a constant print width, allowing square- and round nozzles to print in a continuous and constant track. The addition of optimised structures in the 3D printing process introduces varying print widths, which create the following obstacles:

1. Converting a 2D surface into a 3D printing route (with adjacent print paths).
2. Printing varying print widths on a standard nozzle.

The optimisation process uses solid areas to prescribe a structure. With 3D printing, the goal is to create that same solid structure by printing rows of adjacent concrete, mimicking a solid area. It is uncertain how the printed lanes will behave, if the cohesion is correct, and the effect on the overall stiffness. The step from a digitally optimised structure to a printed structure has to be investigated.

In the virtual world (optimisation process and robot control) is, every element set. Material values are constant, lines are perfect, and the environment is controlled. This is, unfortunately, not the case in the real world. During the process, external elements will affect the process, precision and outcome of the printed structure. This effect has to be taken into account and be expected.

Several things can be done to minimize the effect of the environment. At first, all steps taken are recorded and repeated every printing session. By standardization the process the change of a aberrant result is lowered. Challenges will be tackled before printing sessions, to prevent failures and lost time. Because this is the first time the step from optimization tool to printed structure will be executed, the process will be an ongoing development. Printed structure will have unforeseen errors, which will be improved during the research. Previous studies [5] have presented tools for generating walls/beams with an in-plane loading. This process's main challenge is creating a printed structure that behaves according to the optimised structure.

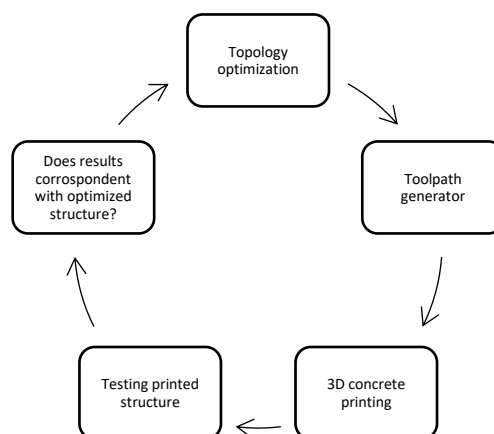


Figure 2 - Challenge

1.3. Research questing

As described in the previous chapter, this research continues previous research focusing on generating walls/beams with an in-plane loading. This research will focus on the validation of the design models.

The following research question is drafted to obtain validation on the models:

“Does a 3D-printed optimised beam have the same structural properties as a optimisation tool prescribed?”

In Figure 3, a step diagram is shown. The diagram shows the difference between the two worlds and the validation between them. The distinction is made between the virtual world(model method) and the real world (printed structure). The validation happens between the design model made with the model method and the printed structure made with a 3DCP.

The optimisation goal is to maximise the system’s performance, but that is not the goal of this research. The goal is to visualise the difference in structural properties between the printed- and optimised structure. A benchmark beam will also be made and tested, to test the improvement (or decline) of the system properties. This benchmark beam is a standard solid beam.

To fulfil the answer to the research question, the printed structure will be compared on several aspects:

- Printed structure compared to the benchmark beam. This will give an insight into the optimisation of the system’s performance.
- Printed structure compared to virtual reality. This will show if the printed structure behaves accordingly to the digital world.

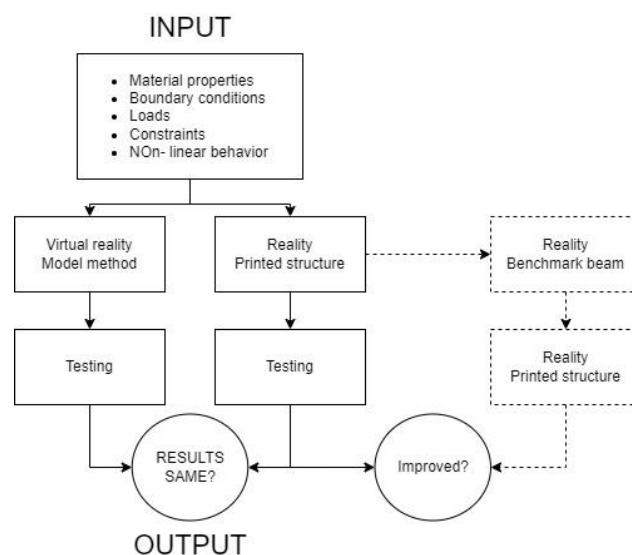


Figure 4 – The challenge

1.4. Thesis outline

The structure of this thesis can be divided into 5 chapters. In this chapter, the subject, challenge and research question are laid-out. The principle of optimisation within this thesis, topology optimisation, is explained. The second chapter, Software Explanation, describes the optimisation process throughout different software programs, from the beginning of the optimisation to the controlling of the robot arm. The printing of the structure is described in chapters 3 & 4. Chapter 3 describes 'How' the structures are printed, whereas chapter 4 describes 'What' structures are printed as case studies. In chapter 5, the results are presented. In chapter 6, a combination of visual- and data comparisons are drawn up to describe the structural behaviour of the printed structure, followed by a discussion of the results. In chapter 7, a total review is performed to answer the main research question.

2. SOFTWARE EXPLANATION

Software programs are used to visualise, create, obtain or control the desired structure from start to end. The cycle of creating and printing the structure is divided into 3 parts: Optimization (green), print path (yellow), and robot control (blue). Every part contributes to the process, from visualising the structure to realising the structure. In this chapter, the software programs used are explained.

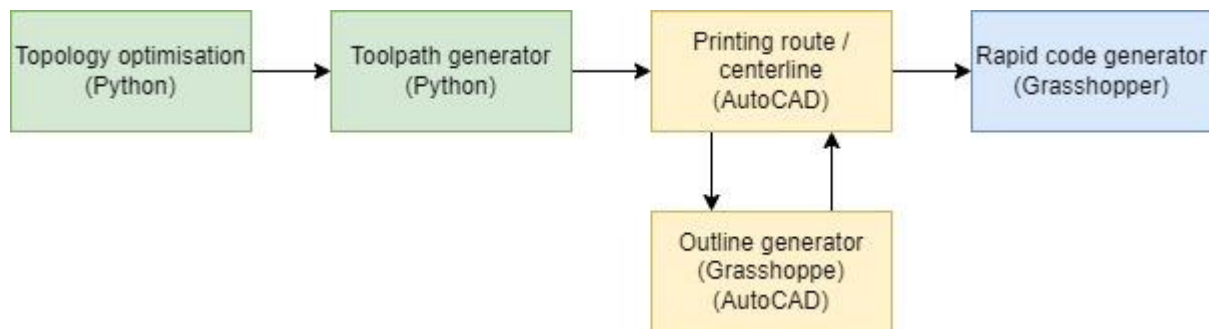


Figure 5 – Software steps

2.1. Topology optimisation (Python)

This research starts with optimising a structure via topology optimisation (TO). A Python script (written by Jelle Versteeg) executes an algorithm that uses a modified SIMP approach (Solid Isotropic Material with Penalization). The algorithm utilises a rectangular 2D domain discretised with square bilinear elements [5].

A stress analysis is incorporated into the algorithm to provide insight into the limit of the structure and its capacity. The script works with a non-linear behaviour of the material to redistribute the forces due to the change of stiffness when the concrete starts to crack. Without non-linear behaviour, the stresses will become unrealistically high in areas loaded in tensile. Stress optimisation can be achieved by two various methods. First is the proportional topology optimisation for stress (PTOs). This method gains simplicity and efficiency at the price of weaker mathematical rigour. The second method is traditional topology optimisation (TTO). This method can optimise solutions that fully utilise the compression strength of the material.

The material model has a modified mohr-coulomb failure surface representing the reinforced concrete. Due to the use of only concrete and no reinforcement, the standard mohr-coulomb failure criterium is used. The results from the TO script can directly imported into the print path script.

2.2. Print path

After designing the structure via the Topology optimisation tools, it's time to determine the print paths to create the optimised structure. The optimisation tool determines where the material is needed, creating a black/white surface. This surface must be divided into print paths, forming the structure's total surface together. The printing route needs to incorporate several aspects. The printed layers cant overlap; they have to include tensile- and compression zones, and a continuous route is mandatory to create multiple layers.

The input for the robot script should obtain two curves, the out- and centreline. These two curves are created via several steps:

- Toolpath generator
- Printing route

2.2.1. TOOLPATH GENERATOR (PYTHON)

The toolpath generator (written by Jelle Versteeg [5]) is divided into 3 significant steps: geometry setup and analysis, member optimisation, and connection optimisation. The script incorporates three requirements [5] that allow 3d printing (reinforced concrete):

- REQ1, a continuous route with identical start and end position
- REQ2, the print path should not intersect itself
- REQ3, for areas of cable-reinforce prints that are loaded in tension, the print path should follow the direction of the tensile stresses as closely as possible

The first part imports the output(.npz file) from the topology optimisation and converts the density array into a polygon, creating a surface with boundaries. After incorporating the boundary conditions, the median axis of the polygon is determined. The second step in the geometry setup is determining the subregions of the polygon that are classified as connections. The distinction between members and connections creates connections with rectilinear surfaces.

The second major step takes a better look at the design of the members. The number of print paths is calculated, incorporating a range of print path widths to determine the optimal number of paths. At last, the reviews of the flow of forces within a connection satisfy REQ3. This step doesn't apply to this research due to using non-reinforced concrete only.

The last step focuses on connection optimisation. The script takes a look at the connection sequences regarding REQ2 and REQ3. These constraints are leading to the search for an optimal printing route.

2.2.2. PRINTING ROUTE(AUTOCAD+GRASSHOPPER)

The second step is creating the out- and centreline from the result of the toolpath script. For this step, AutoCAD is used. Due to the ongoing concrete flow during printing, a continuous printing route is mandatory. This continuous printing route needs to be created by hand.

The result from the toolpath prescribes the number of printing paths, direction, and force within the print paths[step 1]. Connecting the different paths [step 2] creates multiple continuous routes. A single route is needed for printing. This can be obtained by making incisions in 2 different routes [step 3] and forcing the route to make a U-turn. Due to the symmetry of the structure, only half of the structure needs to be assessed. Creating an a-symmetrical structure can result in uncertain behaviour, which is not recommended. If all the steps are executed correctly, the object can be mirrored, creating the desired structure with the needed continuous centreline [step 4].

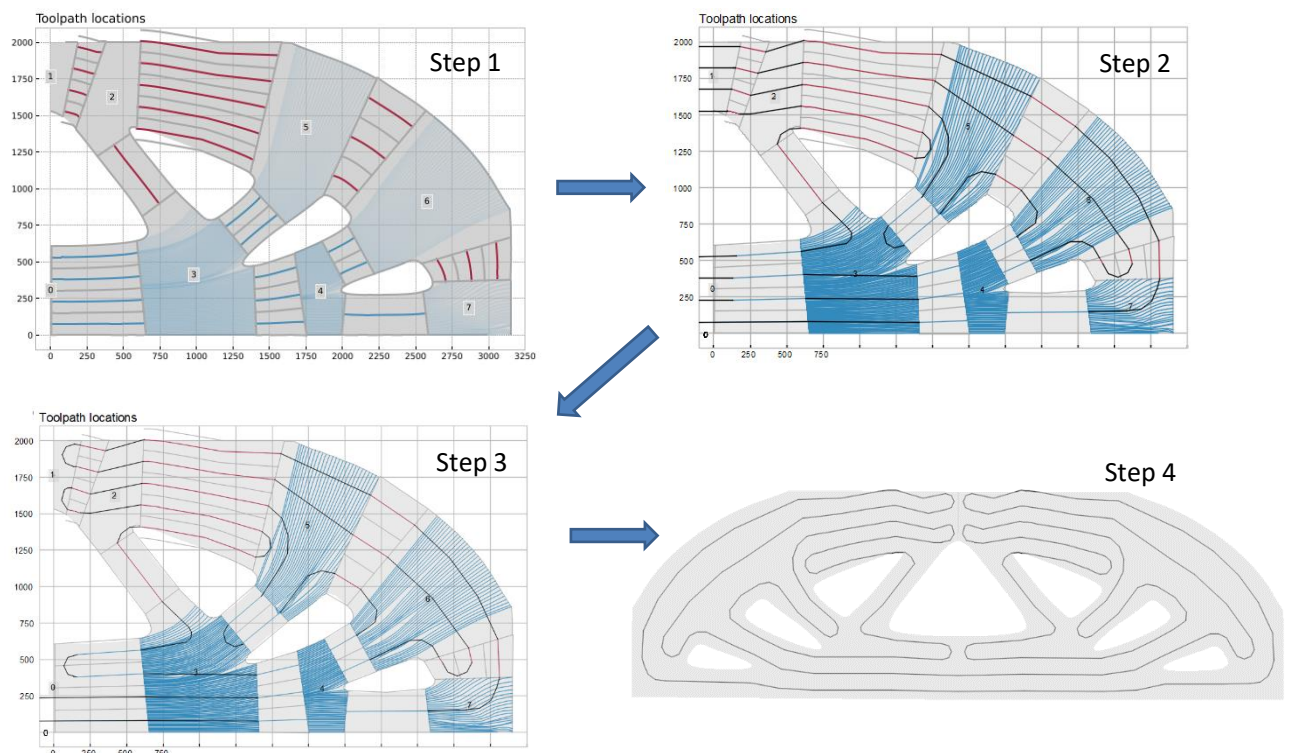


Figure 6 – Printing route

Now that the centreline is established, the outline can be created. Within the grasshopper, the outline is generated using the component Voronoi. The results are exported as a 2d CAD file. This file can be imported within grasshopper to start the next step, generating a Rapid code.

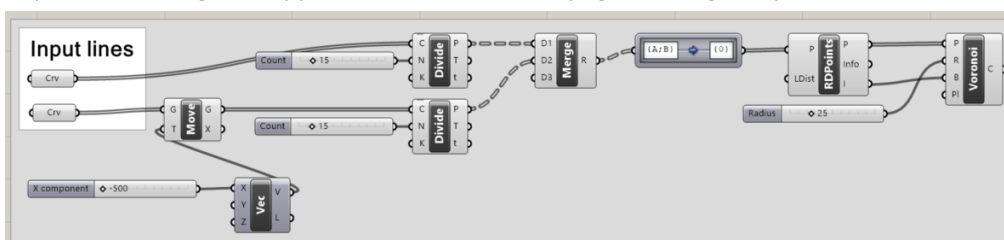


Figure 7 – Grasshopper outline

2.3. Rapid code (Grasshopper)

The previous chapter explains the creation of the centre- and outline. This 2d CAD drawing transforms into a Rapid code that controls the robot arm. The script is divided into 4 phases, each stepping toward the control of the robot arm.

The grasshopper file allows the user to print the structure in 3 different ways. First is the option to print one single object. Secondly is the option to print several objects individually in one printing session (incorporating multiple structures in one rapid code). Last is the possibility to print multiple structures at once, layer by layer, instead of structure by structure.



Figure 8 – Generating rapid code

2.3.1. PHASE 1 – CREATING A LAYERED STRUCTURE

The centre- and outline generated via the print path generator are the starting point for the transformation. After the curves are scaled and repositioned to the desired dimensions, a transformation into a 3d object is made. The curves are multiplied in height, creating single print paths stacked in height instead of one ongoing print path going upwards. A grasshopper component named 'Salad slicer' helps create multiple layers for 3D printing. The component makes an incision in the print path and connects the end of one layer to the beginning of the next layer, creating one long print path with different layers.

2.3.2. PHASE 2 – CREATING COORDINATES + PRINTING SPEED

In phase 2, the centreline transforms from a curve into coordinates for the robot combined with the needed robot speed. This process is divided into 2 stages.

2.3.2.1. *Creating coordinates*

The robot is controlled by moving its local XYZ plane on the end of its arm precisely towards the targeted XYZ plane. The movement of the arm from plane to plane creates a motion representing the print path.

After phase 1, the centreline is still a curve. At first, the curve will be simplified, creating a smaller calculation. Reducing the total amount of data is needed to ensure the software program runs smoothly. If the data remains that large, the software will stall by an overload of calculations. Simplifying the curve has little to no effect on the overall result of the printed structure due to the small size of the printed structure. This simplified curve is then exploded into segments, creating multiple points. These are transformed into planes for the robot to track.

2.3.2.2. Printing speed

The print path generator prescribes a minimum(15mm) and maximum(30mm) width to determine the most optimal printing route. Adjusting the robot's speed between planes can create these deviating widths. The required speed is determined by measuring the closest distance between the centre- and outline the prescribed layer height, and the constant concrete flow of 0,6L/min. The required robot speed is combined with the plane coordinates.

One of the suggested improvements, see chapter 4.2.2.5, is the overlapping of junctions to prevent the appearance of gaps. This results in areas where the centreline almost touches the outline. Grasshopper will analyse this as a small print path width, producing extremely high robot speed. This effect counters the wanted effect of an overlap. A lower bound level(15mm) is incorporated in the script to prevent this from happening, limiting the robot's speed to create solid overlaps.

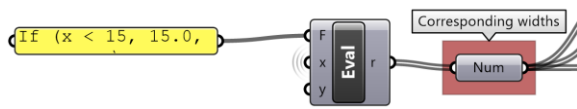


Figure 10 – Lower bound print width



Figure 9 – Overlapping joints

The last part of phase 2 checks if the transformation from a curve to a list of planes combined with the needed robot speed is completed correctly. The print path width is plotted in the upper graft, with the robot speed plotted below. The process is completed correctly if the grafts are mirrored to each other (large width = low speed, and vice versa). Should this not be the case, an error occurred in the process.

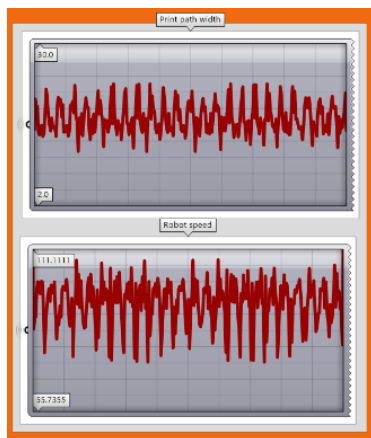


Figure 11 – Width and robot speed

2.3.3. PHASE 3 – PRINTING POSITION

After the coordinates and robot speed are determined, they are transformed into robot targets. These targets are the instruction for the robot on where and how to move. There are 2 different types of movement:

MoveLinear (MoveL) is used to move the tool centre point (TCP) linearly to a given destination at a certain speed.

MoveJoint (MoveJ) is used to move the robot quickly from one point to another when that movement of the TCP does not have to be in a straight line. The robot and external axes move to the destination position along a non-linear path. All axes reach the destination position at the same time. [6]

The prescribed printing routes exterminate the option to use MoveJ. A second downside of using MoveJ is the attached concrete hose to the nozzle. The concrete hose could get stuck if the program suggests rotating an axis 360 degrees.

The first concrete mixing batch isn't suitable for printing. This batch should be pumped through at a position where a bucket can be placed that is not in the way of the printing route. This position will be called bucket start. The concrete pump cannot be paused; thereby, the start of the printing route will be at the bucket.

A distinction is made between the print job of a single structure and multiple structures.

2.3.3.1. *Single structure*

The steps for setting up a single structure are relatively simple. The position of the structure and print bed height are already set in phase 1. The robot targets and speed are obtained in phase 2. The only manual input necessary in phase 3 is the robot's start and end position.

2.3.3.2. *Multiple structures*

When printing multiple structures, different obstacles occur. The first obstacle is the uneven printing bed. The optimum distance between the nozzle and the print should be 8mm. This distance allows the concrete to spread out. A smaller distance results in the concrete being spread out too far, reducing the 6mm height of a layer. If the distance gets larger than 8mm, cracks may occur. A difference in height between the left-(+4mm) and right side (-10mm) has to be incorporated into the positioning height of the structure. By measuring the adjustment can be determined by measuring the height difference between the printing bed and the nozzle for every positioned structure script allows printing different structures in one session. This amount is due to the dimensions of the case study combined with the print bed and robot reach.

The second obstacle to printing multiple structures is the intermediate paths between the structures. The robot cannot go directly from the first structure onto the second. The risks of damaging the structure, pouring concrete all over, or stalling the robot are too great. Prescribed intermediate paths ensure a safe transition from structure to structure. These paths can be created in 2 different manners:

- Incorporating robot targets into the rapid code. These targets can be chosen manually and simply added to the list of coordinates. This option should be used when the input in phase 1 is only one structure, which will later be multiplied and positioned in phase 3.

- The connecting paths can be pre-drawn with AutoCAD. Instead of importing one 2D structure in phase 1, the structure is already multiplied in the CAD file. The intermediate paths are drawn as out- and centrelines and connected to the lines of the structure. This creates one large print route with several structures and intermediate paths. This way of creating intermediate paths has dis- and advantages.
 - Advantage; importing one large print route with several structures allows printing layer by layer instead of structure by structure, thereby allowing the concrete to harden(enough to carry the next layer) between layers.
 - Disadvantage; the internal grasshopper calculation for determining the coordinates and robot speed increases exponentially.

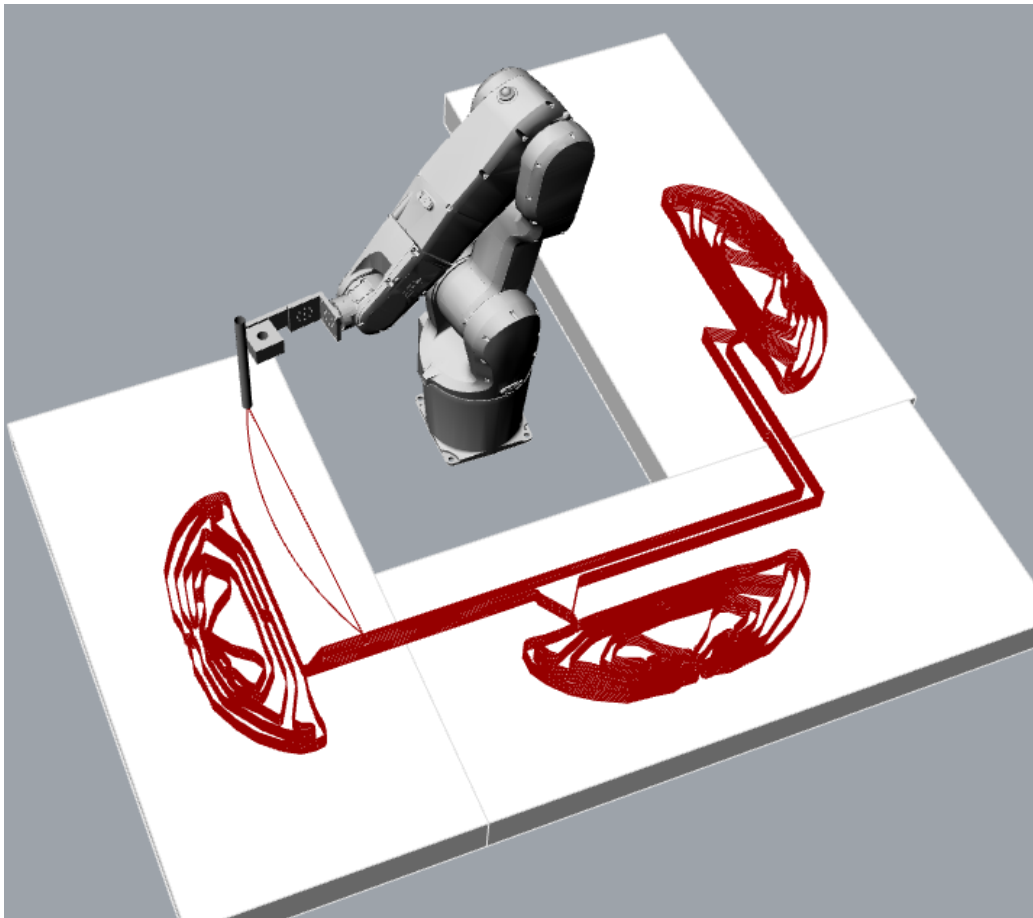


Figure 12 – Virtual printing route

2.3.4. PHASE 4 – CONTROL ROBOT

In phase 4, all the determined coordinates, robot speed, and printing positions are combined and transformed into a file readable for the robot called the Rapid-code. To create the code, the component needs 2 sets of input:

- The info about the robot. This is determined by the specific robot that is used (IRB1200). A nozzle prints the concrete, changing the local XYZ value of the robot's end. Incorporating the nozzle into the component creates a new XYZ value. The robot will align this new value onto the robot targets.
- Robot targets, which hold the coordinates and the desired speed.

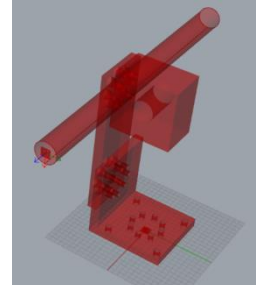


Figure 13 – 3D model nozzle

Once all the data is collected, the Rapid generator creates 2 lists of information.

The first list is a program module. This list contains the coordinates and speed of all the targets. The second list is the system module, which provides the robot cabinet with information about the robot and the tools used.

The final part of phase 4 is operating the robot. A Lan connection between the robot cabinet and a pc has to be established. The Rapid code can be uploaded by copy-pasting the file into the robot settings within Robot Studios. There is also an option to connect the grasshopper and the robot remotely. This allows users to upload the Rapid code directly into the robot without using Robot Studios.

2.4. Karamba (Grasshopper)

The software plugin Karamba is used within Grasshopper to compare the printed- and optimised structures. Karamba3D is a parametric structural engineering tool that accurately analyses spatial trusses, frames and shells. Karamba3D is fully embedded in the parametric design environment of Grasshopper, a plug-in for the 3d modelling tool Rhinoceros [<https://www.karamba3d.com/>].

The grasshopper script is set up in different stages. It starts with importing the centre- and outline. These curves are converted into a 2d surface, combined with the boundaries. The script creates a mesh within the boundaries used for the Karamba calculation. An increased number of nodes increases the accuracy of the calculation.

The mesh is converted into a shell element, providing the calculation with information about the element, supports, loads and cross-section. Once all the information is collected, the Karamba tool analyses the structure and gives the result information. Node information can be extruded via different components to obtain information needed for the comparison.

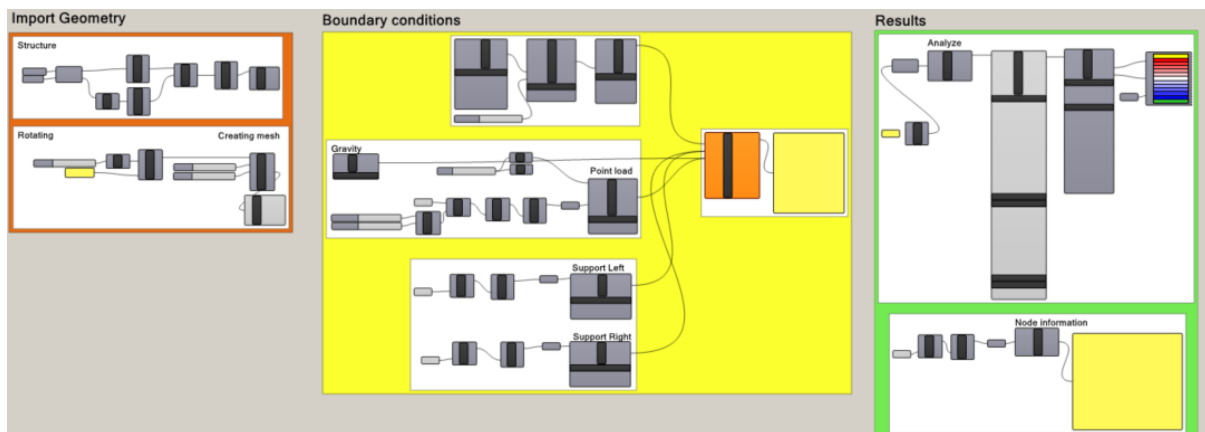


Figure 14 – Karamba calculation Grasshopper

3. METHODOLOGY

3.1. Printing

The 3DPC process is build up out of several, individual elements that combined represent the 3D printer. In this chapter the elements are described for their purpose and their applicability.

3.1.1. PUMP

The concrete pump used for this research is an MAI 2Pumpictor. This small-scale pump is detachable and consists of several components. The concrete enters through a funnel. The electromotor propels a screw at the bottom of the funnel. The screw pushes the concrete through a mould, generating pressure. The rotation speed of the screw can be variated but needs to be set on the lowest velocity. A higher velocity will result in more friction and an increase in temperature, which all lead to solidifying the concrete within the hose. The screw must be lubricated before printing to prevent friction within the mould. A minimum amount of lubricate has to be applied. Too much lubrication results in no friction between the concrete and the screw, which leads to no pressure building up within the hose.

The hose must be flushed with water before attaching it to the pump. Making the inside of the hose wet prevents friction between the concrete and the hose.

A pressure meter is installed at the end of the pump. This meter indicates if the concrete is flowable enough (no pressure) or has started to solidify (high pressure). If, in any case, the pressure builds up, the hose needs to be detached and cleaned directly to prevent the concrete from hardening within the hose.

3.1.2. CCONCRETE

The concrete mixture used for 3D printing is Weber 3D 145-2, C35/45. This mixture is specially developed for 3D printing and has different material properties from standard concrete. The concrete behaves as liquid while mixing/printing but stiffens quickly when printed. This behaviour gives good buildability without the use of formwork. The prescribed water percentage to use is 16%. Throughout the research, a percentage of 16,5% is used, which increased the permeability but didn't affect the buildability. Minor water adjustments (a few drops of water) were made throughout the printing trails to ensure flowability.



Figure 16 – Weber concrete mix



Figure 15 ROASD - 201115 Robots_introduction

3.1.3. ROBOT

This research uses the ABB IRB 1200 robots located at Eindhoven University. A single cabinet operates the robot. The robot has 6 joints that can rotate, giving it almost a 360-degree range. The robot can be operated manually (jogging) or execute a pre-written script (rapid code) following a particular path. The rapid code lines consist of targets, speed, rounding and tool.

The target is divided by an XYZ coordinate. The robot will move the tool to the target to match the tool's local XYZ values with the coordinates of the target. This movement can be executed linearly from point A to B (MoveL) or curved (MoveJ) [6]. To follow the prescribed print path as accurately as possible, MoveL was used.

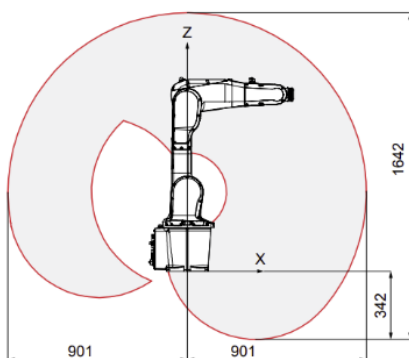


Figure 17 IRB1200 datasheet_220606

3.1.4. NOZZLE

The nozzle consists of an Aluminium clamp and a tube with a connection for the hose. A distance of 6mm is kept between the nozzle and the printing bed during printing. The inner diameter of the tube is 15mm. A round nozzle has the advantage that it can print in any direction without rotating the nozzle. A square

nozzle needs to rotate to follow the curve of the concrete. Because the hose is connected on top of the nozzle, the robot joints can rotate 360 degrees, or the hose will get stuck. With a round nozzle, the XYZ direction of the tool can stay the same while following the curves of the printed structure. A disadvantage of a round nozzle is the spreading of the concrete. This effect is taken into consideration in the optimisation.

3.1.5. PRINTING BED

The concrete is printed on EPS boards placed on the standard printing bed. The printing bed isn't completely horizontal. A height difference of +/- 10mm is present, which must be considered when programming the desired printing route.

3.1.6. CURING

Before the concrete obtains its structural properties, it needs to harden. To prevent the concrete from drying out and developing stresses/cracks, the moisture level in the concrete needs to be maintained. The printed structure must harden for one day before transportation. A plastic sheet sealed off with wet paper towels prevents the printed structure from drying out on the first day. After one day, the printed structure is hardened enough to transport. It will be placed in a container filled with water. The printed structure can continue its hardening process until testing.

3.1.7. SAWING

The supports and measuring tools need to be placed on a flat surface. Elements that don't fit these requirements are sawed to the desired shape. This implies only the top/bottom side horizontally.

3.1.8. GYPS SUPPORT

The structure will be printed on its side and flipped 90 degrees for testing. The edge of the printed structure will be uneven. An uneven surface can cause peak stresses with local failure as a result. To prevent this from happening, a gyps layer is added. Placing the printed structure in a formwork filled with gyps generates a smooth surface. The gyps will spread the stress over the support without contributing to the structural integrity.

3.2. Testing

3.2.1. SETUP

For testing, the Instron Tensile Tester is used. The setup is a 3-point bending test (3PBT), which generates the largest moment in the middle. The centre-to-centre distance between the supports is 600mm. This is the maximum centre-to-centre distance mountable. The beam is simply supported and is free to rotate.

The 3PBT combined with a simply supported beam is chosen for its simplicity in supports. All samples with varying dimensions can be tested within this setup without adjusting anything. The simplicity of the test setup would erase the question if the setup was correct when analysing the results.

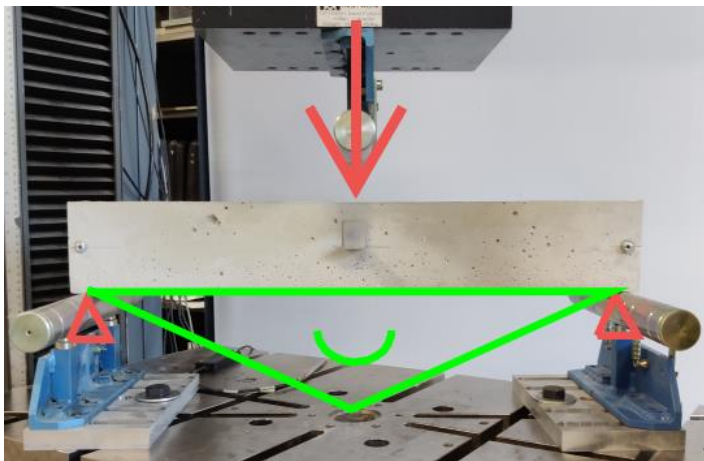


Figure 18 – Test setup

3.2.2. LOAD

A single-point load is used for the 3PBT. This point load is placed in the middle of the structure to generate the largest moment ($1/4FL$). The load applied on the structure is displacement controlled (0,2mm/s), meaning a linear change in displacement which leads to an exponential increase in force. Due to the printed imperfections, a small steel plate is placed on top of the printed structure to spread the forces.

3.2.3. MEASUREMENTS

For the test, several values are measured. The values are measured by the Instron machine or by using LVDT sensors. The linear variable differential transformer (LVDT) is a type of electrical transformer used for measuring linear displacement [7].

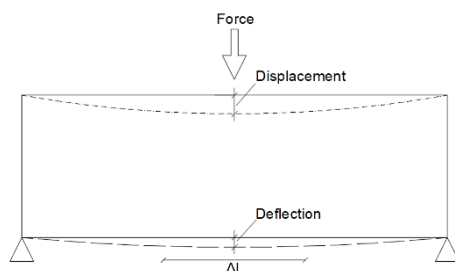


Figure 19 - Measured value

The following values are measured:

- Force, measured via the Instron machine.
- Displacement, this is measured from starting position on top going downwards in a linear increment. The displacement is measured within the Instron machine.
- Deflection, this is measured with 2 separate LDVTs placed on the bottom of the structure. They measure the vertical deflection on the bottom of the structure.
- Elongation, this is measured on the bottom of the structure via an LDVT. The elongation is measured over 120mm in the middle. Via the elongation, the strain can be calculated.
- Rotation, the rotation of the structure at supports is measured using a measuring clock placed on the head of the beam. An increase/decrease in distance implies a rotation. This verifies free rotation at the support.



Figure 20 – LVDT placed on the structure

3.3. Test samples

With every printing session, test samples(160x40x40mm lxbxh) are created with the concrete batch used for printing. The samples undergo a flexure- and compression test on the same day the printed structure is tested. These tested samples indicate the concrete's flexure- and compression strength that day. The flexural strength is determined by a 3PBT(left in the picture). The compression strength via a compression test (middle in the picture). Results are shown on the module(right in the picture). The samples are cured the same way as the printed samples.

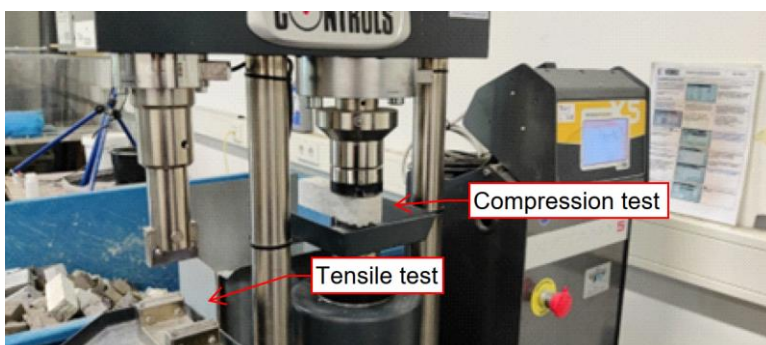


Figure 21 – Sample tester

4. CASE STUDY

Structural optimisation aims to reduce material volume while retaining the optimal structural properties. To determine the change in properties of the optimised structure, solid beams are cast to make the comparison. These beams will be called Benchmark beams. The optimisation, printing, and testing cycle will be executed for the first time. The case study starts with a simple design to narrow the possibility of optimisation-, execution- or data errors. From there out the research can be expanded.

Flaws in the print path optimisation aren't noticeable until the structure is printed. Adjustments are made throughout the case studies to create a printed structure comparable to the optimised structure. Adjustments are made within the optimisation upfront and during execution.

4.1. Topology optimisation input

Within the topology optimisation script, the input is divided into different sections. These settings are decisive in the outcome and process duration of the optimisation.

First are the general script settings. The non-sensitivity optimisation method called proportional topology optimisation for stress (PTO) is used for optimisation. The optimisation is executed in a non-linear calculation to provide the structure to redistribute the forces and prevent the build-up of unrealistically high stresses in areas loaded in tensile [5]. This research uses only concrete and no reinforcement. The uncertain material behaviour of reinforced 3DPC(tensile capacity) [8] creates a difference between the virtual and real worlds, making validation impossible. Here the yield criterion 'Mohr-Coulomb' is chosen. This yield criterion describes the response of brittle material, such as concrete.

Geometrical dimension and material properties are identical for both case studies besides the length and height. Although this project uses specialised 3DPC material, standard C30/37 material properties are used as input. Within the optimisation, the option is given to incorporate gravitational loads. The effect of own weight increases significantly as the volume of a structure decreases (due to optimisation). Incorporating the gravitational loads is therefore recommended.

The optimisation settings are discussed with the creator of the script, Jelle Versteeg. A minimum amount of iterations is set at 50, with a maximum of 90, in the convergence settings. Experience in running optimisations has shown that the script shows little to no improvement beyond +- 100 iterations.

For optimisation, the MBB beam settings are chosen. These settings divided the symmetrical beam in 2, calculating only half the beam. The boundary conditions are:

- Horizontal support = rigid supports all along the cut, with the possibility to translate vertically.
- Vertical support = standard roller, only support vertically. Free in rotation and horizontal translation.

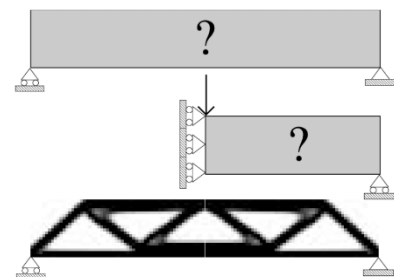


Figure 22 - MBB

4.2. Case 1

4.2.1. BENCHMARK B.1

The beams are cast in formwork with the same concrete used for printing. The advantage of small-scale beams is the weight. They can be manufactured, processed, and tested by a single person without heavy machinery.

4.2.1.1. Dimensions

The length is determined by the limitation in the centre-to-centre distance(600mm) for the supports. A standard dimension ratio for a simple beam is 2/1 (height/width). The dimensions chosen for the Benchmark beam are 630 x 100 x 50mm (Length x height x width).



Figure 23 – Benchmark beam



Figure 24 – Formwork benchmark beam

4.2.1.2. Point load

With the dimensions known, the theoretical strength can be determined. The formulas used for determining the maximum load are:

$$\sigma = \frac{M}{W} \quad W = \frac{1}{6}bh^2 \quad M = \frac{FL}{4}$$

$$\begin{aligned} \sigma &= 3 \text{ N/mm}^2 \\ L &= 600 \text{ mm} \\ b &= 50 \text{ mm} \\ h &= 100 \text{ mm} \end{aligned}$$

$$F = \frac{\sigma * bh^2}{\frac{1}{4} * \frac{1}{6} * L} = \frac{3 * 50 * 100^2}{1,5 * 600} = 1,66kN$$

4.2.2. 630X100

4.2.2.1. Dimensions

The first printed structure is optimised within the dimensions of the benchmark beam. The printed structure consists of 8 layers. Each layer has a height of 6mm, making the total width 48mm. This reduced cross-section will result in a lower strength. This effect needs to be taken into account when analysing the results.

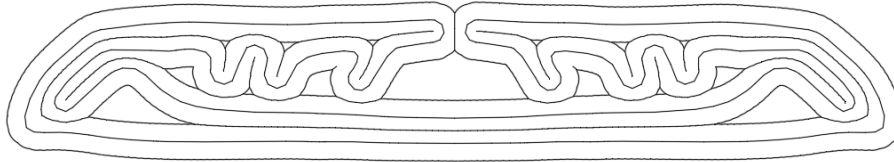


Figure 25 – Centre- and outline 630x100 beam

4.2.2.2. Point load

The theory prescribes the maximum point load for the benchmark beam. This value is used for the optimisation of the printed structure. Unfortunately, this force results in an error within the python script, meaning there is no solution for optimisation with the given input. The force is reduced step by step to find a value where optimisation is possible.

The force where optimisation is possible is 0,35 kN. This is almost 5 times smaller than the theoretical benchmark strength, 1,66kN. The reason for the error within the optimisation is uncertain due to the origin. The TO script uses a pre-written topology optimisation formula. The error appears in that area of the script. Due to a lack of knowledge of this formula, it cannot resolve this error.

Without a solution for the error, it is possible to explain. The magnitude of the optimisation is determined by several factors, namely material properties, supports, and dimensions. The height of this structure gives little room for optimisation. The limited height prevents the TO-script from creating a compression arch.

4.2.2.3. Printing

The 630x100 beam is the first optimised printed structure with the small ABB robot. Every structure is printed separately, as shown in picture 27. A total of 6 beams were printed, but during the process, 1 beam collapsed.



Figure 26 – Printing first 630x100 beam

The first beam is printed with the prescribed speed (100%) generated within the grasshopper script. There is a noticeable visual difference between the optimised and printed structures. Several printed lines don't connect, altering the structural behaviour.

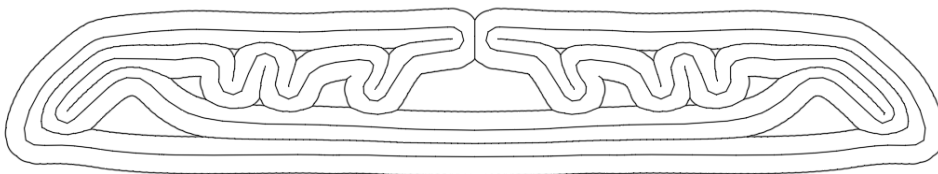


Figure 27 - Centre- and outline 630x100 beam



Figure 28 – Tested 630x100 beam (100%speed)

The robot speed is manually reduced for printing the remaining 4 beams. Reducing the robot's speed increases the time to print the entire structure. The decreased robot speed and constant concrete flow create a wider printing layer. The robot speed is reduced to 90% for 3 structures and 80% for 1 structure.

The reduced robot speed creates a printed structure more similar to the optimised structure. This alteration in execution (increase in weight) must be considered in the results.



Figure 29 – Tested 630x100 beam (80%speed)

4.2.2.4. Continuous printing route

A continuous printing route must be created to print the structure in one section. This is obtained by creating a cut in the printing route, forcing the route to make a U-turn. The amount of U-turns needed depends on the number of layers.

The total amount of layers that create the height of the beams is always a multitude of 2. The minimum amount of cuts can be calculated via the formula:

$$\text{Amount of cuts} = \frac{n}{2} - 1$$

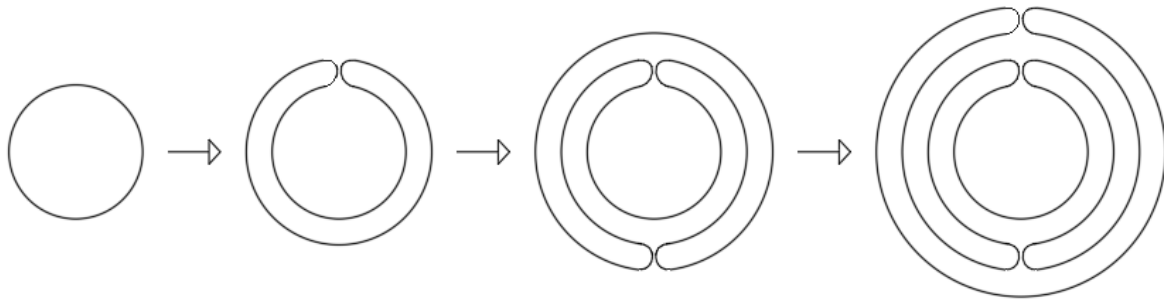


Figure 30 – Continuous path with layers+cuts

Example 1:

The printing route on the right in the picture seen above has 8 layers. The formula states:

$$\text{Amount of cuts} = \frac{8}{2} - 1 = 3$$

Example 2:

The printing route in the first case study has 4 layers. The formula states:

$$\text{Amount of cuts} = \frac{4}{2} - 1 = 1$$

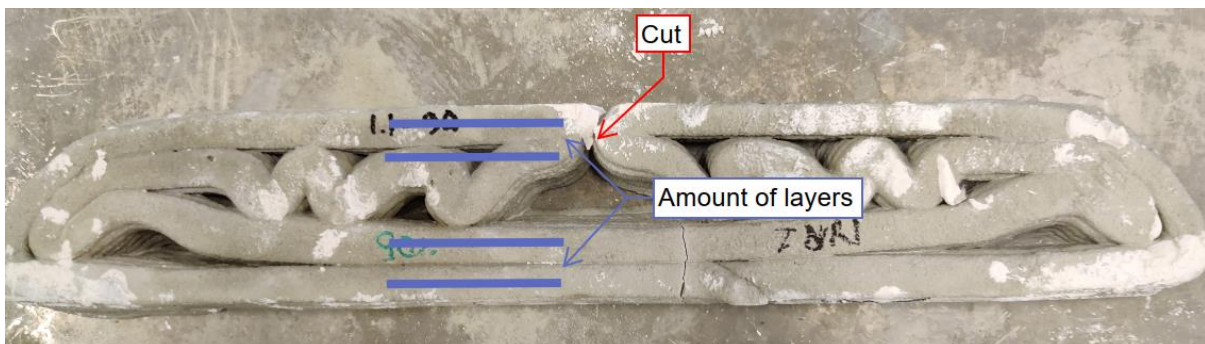


Figure 31 – Example layers+cut

4.2.2.5. Suggested improvements

The first noticeable flaw after printing is the gap at the position of the cut. The layers don't connect, altering the structural behaviour. A temporary fix is made, and a solution for further printing sessions is implemented:



Figure 32 – Imperfection after printing

- Fixture, a layer of gyps is applied in between the gap. The printed structure is set to fail due to tensile stresses. The force needed for the failure of the beam is lower than the maximum compression strength of the gyps. The gyps layer can endure the compression stresses without breaking or altering the structural properties.
- Solution, this flaw can be prevented within the print path script. Previously the layers would be connected from the outline, which results in a gap. Instead of connecting the outlines, the centrelines should be connected, creating an overlap. A 50% overlap provides enough extra material to separate the intersection and create an even cross-section.

The required robot speed is determined by the closest distance between the centreline and the outline, as described in chapter 2.3.2. The grasshopper script will determine a very small distance (until there is no distance between the centrelines), generating a very high robot speed (a faster robot speed creates thinner printing lines). This effect is not preferable. A lower limit (7,5mm) distance between the centreline and outline is built into the script. This prevents the robot from going too fast while printing an overlap.

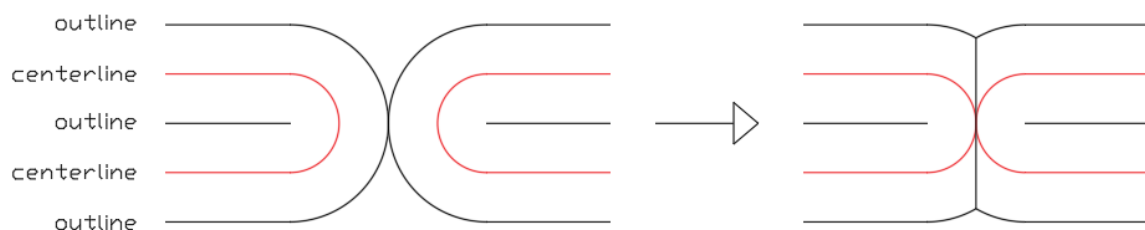


Figure 33 - Overlapping joints

4.3. Case 2

An enlargement of the first case study is chosen for the second case study. This case study consists of one benchmark and 2 printed structures. The printed structures are generated from the same topology optimisation output but processed via different print path methods.

The height of the structure is doubled, creating a 630x200x50mm structure. The extra height creates a larger internal lever arm, lowering the tensile stresses compared to case study 1. The extra height gives more freedom for the TO script, resulting in better optimisation. For example, the script can create a compression arch, lowering the tensile stresses, which is preferable when working with unreinforced concrete.

The test setup can remain the same when increasing the structure's height. A clear analytic comparison can be drawn between the two case studies by adjusting only one variable in the test (namely, the height).

4.3.1. BENCHMARK B.2

Another benchmark beam is chosen to test for this case study. The results from the benchmark can be used directly to compare this case study and the previous case study.

Due to the simplicity of the benchmark beam, an accurate prediction of the result can be determined with the literature. Should the tested results deviate from the expected results, an error within the test setup is possible. If the tested results come near the predicted results, it can be stated that the test setup represents the correct schematisation.

4.3.1.1. Point load

The maximum theoretical load can be determined via the same formula previously used. Within the formula for the section modules, the height is presented to the power of 2. The maximum load increases quadratically if the height is increased. This shows that the structure's height is important in determining the maximum strength.

$\sigma=3\text{N/mm}^2$
 $L=600\text{mm}$
 $b=50\text{mm}$
 $h=100\text{mm}$

$$F = \frac{\sigma * bh^2}{\frac{1}{4} * \frac{1}{6} * L} = \frac{3 * 50 * 200^2}{1,5 * 600} = 7,22\text{kN}$$

4.3.2. 630X200 V.1

As with benchmark b.2, the height for the 630x200 v.1 beam is doubled compared to the first case study. The structure is generated via the same method. All variables are kept the same except the height and point load.

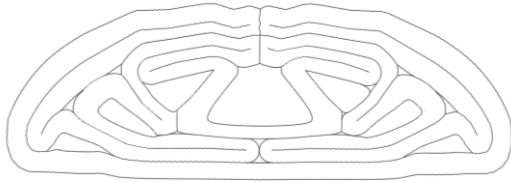


Figure 34 – Centre- and outline 630x100 v.1



Figure 35 – 630x100 v.1 printed structure

4.3.2.1. Point load

A point load of 20kN is chosen as input for the topology optimisation. The reason for deviating from the calculated maximum load of 7,22kN is the prescribed structural outcome. The software prescribes a very low amount of material combined with a few structural ribs. This leaves only a small area for optimisation within the print path generator.

Increasing the load results in a larger volume and more structural ribs, giving more space for the optimisation process. The increased amount of connections creates a greater implementation challenge.



Figure 36 – optimization 7,22kN



Figure 37 – Optimisation 20kN

4.3.2.2. Printing

Contrary to the first printing session, all 6 beams are printed via one large Rapid-code in a single printing session. This printing provides a continuous workflow, resulting in a constant behaviour of the concrete. All layers of one beam are printed at once before going onto the next beam.



Figure 38 – Printing 630x100 v.1

4.3.2.3. Suggested improvements

In the second printing session, several design/execution flaws came to service. Each flaw will be viewed and processed for improvement during upcoming printing sessions.

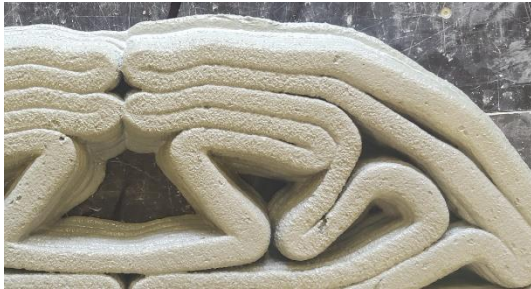


Figure 39 – Imperfection 630x100 v.1

1. The first and last printing layers deviate in width, with the first layer being the widest. With every additional layer, the width narrows down, creating a cone-like section. This is problematic during testing. A flat surface is required to apply the point load.
 - Fixture, a flat surface can be obtained by trimming the printed structure. A concrete saw can trim the beam's top and bottom parts. The superfluous material can be removed without intervening with the structural behaviour of the printed structure.
 - Solution A) the beams are printed one by one, leaving little hardening time in-between printing layers. Instead of printing all layers of one beam once, one layer of all beams should be printed before continuing to the next layer. The hardening time is due to this increase, allowing the printed layer to support the weight of the upcoming layers. B) the first batch of concrete pumped through the hose has an increased percentage of water content to reduce friction and prevent blockage. Using this concrete can reduce the buildability, resulting in layers that expand upon load. Waiting until the first mixing batch goes through the hose and nozzle before starting the printing route is recommended for future printing sessions.

2. Some intersections, parallel print paths, and joints don't connect completely with each other. To validate the optimisation software, the printed should resemble the optimised structure as accurately as possible to achieve the structural behaviour as predicted.
 - Fixture, no fixture is possible to connect/fill the gaps. The results after testing will determine the effect of these gaps.
 - Reason for this problem is the obtained centreline combined with the adjustable robot speed. The distance between the 'centre 'line and the left/right outer line should be the same. This was not the case during this printing session. The steps for generating the outer- centreline are: Results PP → generating centreline → generating an outline. The outline is generated with the grasshopper component Veronoi. This component creates a boundary around a certain point. The radius of the boundary can be increased until it reaches another boundary. Unfortunately, the component doesn't stop if a

boundary is reached. The component creates an uneven radius to enlarge the boundary, creating two different distances between the centre- and outline.

- Solution, an extra step should be taken to obtain the outer- and centreline. After generating an outline, a new centreline is needed. This new centreline is generated from the outline to create an actual 'centre' line, where the distance between the centre- and outline is equal on both sides.

4.3.3. 630X200 V.2

All suggested improvements are incorporated in the second version of the 630x200 beam. Connections are manually adjusted to create an overlap, correct centrelines are created, and adjustments in execution are made.

4.3.3.1. *Print path*

The predicted failure mechanism with a 3-point bending test is a crack in the middle of the lower part of the printed structure. The maximum tensile strength will be reached due to the increasing bending moment, which has its maximum value in the middle.

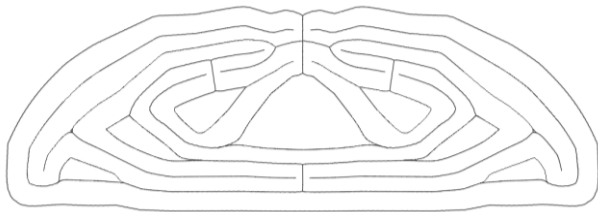


Figure 40 – Centre – and outline 630x100 v.2



Figure 41 – 630x100 v.2 printed structure

Intersections and joints are vulnerable to imperfections during printing. To decrease the possibility of execution, intersections and joints should be minimised within the weakest parts of the structure. Printed concrete without reinforcement has an extremely low theoretical tensile strength (3N/mm^2) compared to compression strength (30N/mm^2). For that reason, intersections and joints should be placed outside the tensile regions of the structure.

All joints and intersections are placed outside the tensile region for the second version, except for one. Creating a symmetrical structure without placing an intersection at the lower part is impossible.

5. RESULTS

After a minimum curing period of 8 days, the printed- and casted structures are ready to be tested via a 3point-bending(3PBT) test. The test is conducted via an Instron Tensile Tester. The measured results are exported in Excel and assembled into an overview.

In this chapter, the results will be summarised and reviewed. Comparisons will be drawn from the tested benchmark, printed structures, and numerical results.

5.1. Result

Results are generated via the 3-point bending test with the Instron Tensile Tester. The data collected via this test are processed and summarised into an overall test result scheme. The following values are measured in these tests:

- Force
- Displacement (top of the structure)
- Deflection (bottom of the structure)
- Elongation (middle bottom)

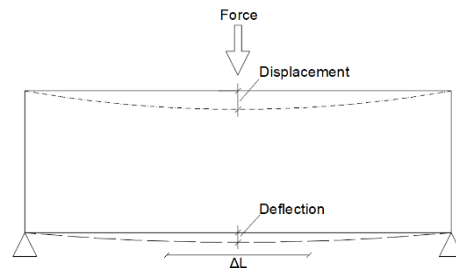


Figure 42 - Measured values

After every printing session, small test samples are made from the remaining concrete. These samples are tested on the same day as the printed structures to give an insight into the material properties of the concrete when the printed structures are tested. The values generated are an indication of the compression- and tensile strength.

3.1.2. DATA

The first data point set is the values from the printed- and casted structures. The values of the digital- and experimental tests are summarised in an overview:

		Experiment data												Software data									
		Force (kN)	Prescribed force (kN)	Displacement max (mm)	Displacement max (mm)	Deflection max (mm)	Displacement 2kN (mm)	Deflection 2kN (mm)	Displacement 5kN (mm)	Deflection 5kN (mm)	Δl (mm)	Days old	Comp. strength (Mpa)	Flex. strength (Mpa)	Weight (kg)	Printingspeed (%)	Weight 100% (kg)	Weight T0 (kg)	Weight PP (kg)	Displacement Karamba	Deflection Karamba		
E30x100 benchmark	b1.1	1.215	1.66	1.68	0.204	0.204																	
	b1.2	1.215	1.66	0.893	0.106	0.106																	
	b1.3	1.638	1.66	0.752	0.158	0.158																	
	b1.4	0.858	1.66	0.614	0.209	0.209																	
	b1.5	1.173	1.66	1.569	0.251	0.251																	
	b1.6	0.987	1.66	0.892	0.287	0.287																	
E30x100	1.1	2.837	0.350	1.557	0.514	1.328	0.366	0.050	20.000	48.070	4.860	5.827	5.310	6.431	80%	5.145	6.240	6.719					
	1.2	2.635	0.35	1.486	0.305	1.344	0.224	0.049	20	50.650	4.860	5.928	5.335	6.062	90%	5.456							
	1.3	3.114	0.35	1.280	0.525	0.985	0.325	0.050	20	51.830	4.860	6.037	5.433	6.037	90%	5.433							
	1.4	3.233	0.35	1.884	0.876	1.491	0.590	0.038	20	51.640	37.300	5.179	100%	5.179	100%	5.179							
	1.5	2.311	0.35	1.396	0.471	1.305	0.411	0.046	20	37.300													
E30x200 benchmark	b2.1	12.526	7.27	1.372	0.995	0.995	0.776	0.533	0.046	17	46.757	7.250	13.359	7.250	13.359					1.130	0.924		
	b2.2	-13.383	7.27	1.504	1.248	1.248	0.835	0.753	0.050	17	45.940	7.030	13.487	7.030	13.487								
	b2.3	-10.226	7.27	1.108	0.910	0.910	0.821	0.337	0.050	17	46.080	6.820	12.893	6.820	12.893								
E30x200 v1	2.1	7.870	20	1.472	0.482	1.220	0.316	0.034	17	46.392	4.456	11.167	10.051	4.456	11.167					11.996	12.975	0.611	0.402
	2.2	8.291	20	1.302	0.484	1.016	0.319	0.032	17	43.520	4.470	11.423	10.281	4.470	11.423								
	2.3	7.889	20	1.473	0.473	1.238	0.317	0.040	17	46.420	3.530	11.368	10.231	3.530	11.368								
	2.4	6.876	20	1.264	0.345	1.124	0.256	0.040	17	46.470	5.070	10.352	9.317	5.070	10.352								
	2.5	8.231	20	1.684	0.539	1.425	0.371	0.023	17	48.560	3.760	11.327	10.194	3.760	11.327								
	2.6	5.546	20	1.485	0.539	1.435	0.494	0.034	17	49.040	3.830	10.457	10.457	3.830	10.457								
E30x200 v2	3.1	13.087	20	2.222	1.345	1.388	0.794	0.024	10.5	43.573	6.132	11.482	11.452	6.132	11.482					11.996	12.975	1.064	0.699
	3.2	13.189	20	1.627	1.228	0.780	0.501	0.023	11	51.490	7.910	11.271	11.271	7.910	11.271								
	3.3	12.822	20	2.598	1.366	2.598	1.573	0.021	11	48.890	7.130	11.584	11.584	7.130	11.584								
	3.4	14.630	20	3.076	1.875	1.490	0.802	0.033	10	38.740	5.460	11.600	11.600	5.460	11.600								
	3.5	12.793	20	2.341	1.566	1.422	0.668	0.020	10	39.620	6.140	11.398	11.398	6.140	11.398								
	3.6	11.576	20	1.641	0.875	0.985	0.405	0.021	10	32.180	5.250	11.322	11.322	5.250	11.322								

Table 1 – Results of experiment and software

There are 2 sets of deflection and displacement showed. First are the maximum values, measured at the peak load of the structure. Second are the values halfway through the test, to give an insight of the displacement while the concrete is behaving in a linear-elastic way.

The second set of data points is the results from the test samples. The measured kN is converted into Mpa values to give insight into the test samples' flexure- and compression strength. The Mpa values are obtained via the following formulas:

- Compression : $\sigma_c = \frac{F}{A}$ example: $\sigma_c = \frac{74,16 \cdot 10^3}{40 \cdot 40} = 46,34 \frac{N}{mm^2}$
- Flexure : $\sigma_t = \frac{M}{W} = \frac{\frac{1}{4}FL}{\frac{1}{6}bh^2}$ example: $\sigma_t = \frac{\frac{1}{4} \cdot 2,07 \cdot 10^3 \cdot 100}{\frac{1}{6} \cdot 40 \cdot 40^2} = 4,86 N/mm^2$

Average values	Compression		Flexure		Time
	kN	Mpa	kN	Mpa	Days
630x100	74,16	46,34	2,07	4,86	20
630x200v1	71,41	44,57	1,85	4,35	17
630x200v2.1	80,49	50,30	3,18	7,45	11
630x200v2.2	58,96	36,85	2,40	5,62	10
B.2	74,82	46,76	3,10	7,25	17

Table 2 – Results of test samples

There are multiple curiosities within the test samples results, namely:

- The v.1 samples are in accordance (both in tensile- and compression strength) with the first printing session, the 630x100 beam. However, the v.2 and B.2 values are significantly higher.
- V2.1 and v2.2 are printed with a one-day difference, but v.2.1 has a flexure capacity of 25% higher. This difference is not noticeable in the maximum failure load results per structure. Whether the flexural capacity tends towards the v2.1 results, to the v2.2 or an average value is uncertain.
- The strength capacity differences between v2.1 and B.2 are relatively close, but the hardening time differs by one week. This suggests that the strength capacity of the v2.1 printed structures will transcend the B.2 material properties.

The test sample data shows an uneven result in strength development. This effect must be incorporated in the strength assessment of the printed structures. There are multiple possible reasons for the differences in strength development:

1. There can be a difference in cement composition between the cement bag batches, which affects the material properties. Previous experience has shown different concrete behaviour. This reason is plausible for the differences between case studies. This was unlikely during the v2.1 and v2.2 printing sessions because they were the day after each other.
2. The amount of water used for the concrete mixture greatly affects the printed concrete's overall behaviour. A slightly inaccurate water percentage may be used during printing (wrongly measured or vaporised during the process).
3. Excess concrete is placed in steel moulds after printing the structures to create the test samples. These moulds are covered with a plastic sheet to prevent vaporisation. A puncture in the plastic sheet or a breached seal can cause moisture to escape and affect the hardening of the concrete.

6. COMPARISON AND DISCUSSION

After the data is collected, sorted, and presented in an overview, its time to compare the data and analyse the results. There are several levels of comparison when analysing such large amounts of data. Comparisons can be drawn between the results from the tested benchmark-printed structures and numerical results.

In this chapter, four different comparisons are worked out as examples. The way these comparisons are conducted can be applied to all the data. The following comparisons are executed as an example:

Comparison:	Series used for comparison:
Comparing results within series (Blue)	630x100
Comparing results between series (Yellow)	630x200 benchmark 630x200 v.1 630x200 v.2
Comparing prescribed weight vs measured weight (Red)	All printed series
Experimental results vs numerical results (Green)	630x200 benchmark 630x200 v.1 630x200 v.2

Table 3 - Overview comparisons

Experiment data											Software data				
	Force (kN)	Prescribed force (kN)	Displacement (mm)	Deflection (mm)	dL (mm)	Days old	Comp. strength (Mpa)	Flex. strength (Mpa)	Weight (kg)	Printingspeed (%)	Weight 100% (kg)	Weight TO (kg)	Weight PP (kg)	Displacement Karamba	Deflection Karamba
630x100 benchmark	1,202	1,66	1,168	0,204					7,358						
b1.1	1,215	1,66	0,893	-0,106					7,358						
b1.2	1,638	1,66	0,752	-0,158					7,358						
b1.3	1,344	1,66	2,286	-0,213					7,358						
b1.4	0,858	1,66	0,614	-0,209					7,358						
b1.5	1,173	1,66	1,569	-0,251					7,358						
b1.6	0,987	1,66	0,892	-0,287					7,358						
630x100	1,023	13,51435	0,184	0,598	0,036	15,67391	46,295	5,797	10,355		9,341	6,240	6,719		
1.1	2,635	0,35	1,486	-0,305	0,049	20	50,650		6,431	80%	5,145				
1.2	2,890	0,35	1,736	-0,393	0,066	20	53,930	4,860	5,928	90%	5,335				
1.3	3,114	0,35	1,280	-0,393	0,066	20	51,830		6,062	90%	5,456				
1.4	3,233	0,35	1,884	-0,876	0,038	20	51,640		6,037	90%	5,433				
1.5	2,311	0,35	1,396	-0,471	0,046	20	37,300		5,179	100%	5,179				
630x200 benchmark	12,526	7,27	1,372	0,995	0,046	17	46,757	7,250	12,723					1,130	0,924
b2.1	-13,383	7,27	-1,504	-1,248	0,050	17	45,940	7,030	13,487						
b2.2	-13,969	7,27	-1,504	-0,827	0,050	17	46,080	6,820	12,275						
b2.3	-10,226	7,27	-1,108	-0,910	0,037	17	48,250	7,900	12,407						
630x200 v1	7,870	20	1,472	0,482	0,034	17	46,392	4,456	11,167		10,051	11,996	12,975	0,611	0,402
2.1	8,291	20	1,302	-0,484	0,032	17	43,520	4,470	11,423	90%	10,283				
2.2	8,065	20	1,635	-0,570	0,035	17	46,990	5,450	11,367	90%	10,230				
2.3	7,889	20	1,473	-0,473	0,040	17	46,420	3,530	11,368	90%	10,231				
2.4	6,876	20	1,264	-0,345	0,040	17	46,470	5,070	10,352	90%	9,317				
2.5	8,231	20	1,684	-0,539	0,023	17	48,560	3,760	11,327	90%	10,194				
2.6	5,546	20	1,485	-0,539	0,034	17	49,040	3,830	10,457	100%	10,457				
630x200 v2	13,087	20	2,222	1,345	0,024	10,5	43,573	6,532	11,452		11,452	11,996	12,975	1,064	0,695
3.1	-13,169	20	-1,027	-1,228	0,025	11	51,490	7,910	11,271	100%	11,271				
3.2	-13,510	20	-2,051	-1,220	0,026	11	50,520	7,300	11,537	100%	11,537				
3.3	-12,822	20	-2,598	-1,366	0,021	11	48,890	7,130	11,584	100%	11,584				
3.4	-14,630	20	-3,076	-1,875	0,021	11	48,890	7,130	11,584	100%	11,584				
3.5	-12,793	20	-2,341	-1,506	0,020	10	39,620	6,140	11,398	100%	11,398				
3.6	-11,576	20	-1,641	-0,875	0,021	10	32,180	5,250	11,322	100%	11,322				

Table 4 – Comparisons of data

6.1.1.1. COMPARING RESULTS WITHIN SERIES

The first comparison looks at printed structures with the same measurements. This is useful to determine an average value. Deviating values can point to flaws during printing or testing.

Five printed structures with the dimension of 630x100mm are tested. In the table below, the results from the test are compared with the measured weight. Beam 1.1 is printed with a robot speed of 80%. Beams 1.2, 1.3 and 1.4 are printed at 90% robot speed, and beam 1.5 is printed fully at the prescribed speed, namely 100%. These different robot speeds need to be considered while comparing the results.

The choice to adjust the robot speed between printing sessions comes from the visual observation during the printing. With the prescribed robot speed of 100%, the structure seemed insufficiently connected at joints and had an overall slender appearance. Reducing the robot speed increases the printing time, resulting in more concrete (since the concrete flow is constant). The speed is reduced twice. With a robot speed of 80%, the total surface area overwrites the prescribed area. A robot speed of 90% resulted in the most similar area as prescribed.

6.1.1.1. Comparison

	kN	kg	kN/kg	Printingspeed (%)	Deviation force compared to average	Deviation weight compared to average	deviation kN/kg compared to average	% deviation compared to average
630x100	2,837	5,802	0,496					
1.1	2,635	6,431	0,410	80%	-7,1%	2,2%	-0,008	-1,7%
1.2	2,890	5,928	0,488	90%	1,9%	2,2%	-0,008	-1,7%
1.3	3,114	6,062	0,514	90%	9,8%	4,5%	0,018	3,6%
1.4	3,233	6,037	0,536	90%	14,0%	4,1%	0,040	8,0%
1.5	2,311	5,179	0,446	100%	-18,5%	-10,7%	-0,050	-10,0%

Table 5 – kN/kg 630x100

The first values to compare are the failure loads, the weight, robot speed and the force per kg weight. Due to changes in printing speed, the total weight per printed structure varies. An indication suggests that the weight increase resulting from the adjusted robot speed results in an increase in failure load (90% vs 100% printing speed). Printed structure 1.1, printed at 80%, counters this suggestion. The results show that the highest kN/kg values are achieved by the structures printed at a 90% robot speed. It can't be stated that more weight results in a higher failure load*.

*This suggestion is checked for every case study. All case studies found samples that didn't match the suggestion.

It's more likely that the highest failure load can be found at an optimal weight configuration, as designed with the TO script. Structures printed at 80% (+3%) and 90%(-3%) show a difference of 3% in weight compared to the prescribed weight from the TO script. This suggests the expectation that the kN/kg ratio would be around the same value, but 80% shows a 20% lower kN/kg ratio. This suggests that other aspects significantly impact the kN/kg ratio, or once the printed weight surpasses the prescribed weight, the kN/kg ratio diminishes exponentially.

As expected, the concrete properties at the moment of testing show no deviation within the series of test samples because the test samples are made from the same concrete batch.

	Displacement 2kN	Deflection 2kN	kN	kg	disp/ kg	defl/ kg	kN/kg	defl/ disp
630x100	1,328	0,366	2,8366	5,802	0,225	0,063	0,496	27,8%
1.1	1,344	0,224	2,635	6,431	0,209	0,035	0,410	16,6%
1.2	1,516	0,280	2,890	5,928	0,256	0,047	0,488	18,5%
1.3	0,985	0,325	3,114	6,062	0,163	0,054	0,514	33,0%
1.4	1,491	0,590	3,233	6,037	0,247	0,098	0,536	39,6%
1.5	1,305	0,411	2,311	5,179	0,252	0,079	0,446	31,5%

Table 6 – Deformation 630x100

The values for displacement, deflection, and elongation, as described at the beginning of this chapter, can indicate the stiffness of a printed structure. A printed structure with a high stiffness behaves more like a rigid body (as the benchmark) with a uniform deformation. Differences between displacement and deflection indicate a low stiffness. Rotational possibility, incorrect joints and local deformation within the printed structure can be the reason for a lower stiffness.

There is no direct connection between the displacement and the total weight of the structure. Structure 1.1, printed at 80% robot speed, with the highest own weight, doesn't show deviating values compared to the 90% robot speed printed structures. Where the structures showed an optimal force/weight ratio at 90% robot speed, no connection is found between the displacement weight of the structure. (structures 1.1, 1.4 and 1.5 counter any correlation between displacement and weight) .

6.1.1.2. Statements

Comparing the results of the printed beams between themselves, implement the following observation statements:

1. Although at first sight, the data suggest that an increase in weight also increases the failure load, some data points counteract this statement. (beam 1.1)
2. Structures with higher defl/disp can endure higher loads with the same displacement. (beam 1.1 compared to 1.3 and 1.4)
3. Combining a high volume with a high defl/disp value resulted in the highest failure load. Printed structures with solely a high volume or a high defl/disp value underperformed. This suggests that a combination of the two values results in the overall performance and failure load of the printed structure:
 - beam 1.2: high kg, low defl/disp → low kN
 - beam 1.4: high kg, high defl/disp → high kN
 - beam 1.5: low kg, high defl/disp → low kN

6.1.2. COMPARING RESULTS BETWEEN SERIES

Optimisation aims to maximise the performance of the system relative to the overall weight of the system. This means topology optimising a solid beam by removing material while optimising its structural property. The optimisation effect can be visualised by comparing the optimised structure with the original design, a solid beam.

This chapter compares the benchmark b.2 solid beams to the optimised 630x200 printed structure. Optimised structures v1 and v2 will both be taken into comparison. V2 is an improved version of v1. The effect of the imposed improvements is visible in the results.

6.1.2.1. Comparison

	Displacement 5kN	Deflection 5kN	kN	kg	disp/ kg	defl/ kg	kN/kg	defl/ disp
630x200 benchmark	0,776	0,533	12,526	12,723	0,061	0,041	0,985	0,690
630x200 v1	1,220	0,316	7,483	11,049	0,114	0,031	0,677	0,275
630x200 v2	1,388	0,734	13,087	11,452	0,121	0,064	1,143	0,517

Table 7 – Results 630x200

The kN/kg ratio first indicates the structure’s overall strength. Noticeable is the average 1,143kN/kg value for the v2 structure. This value suggests the v2 printed structure has a higher load per own kg of mass. This contradicts the statement made at the start of this project:

‘A structure cant increase in strength by decreasing in volume.’*

The statement needs to be corrected when following the values from the Instron tensile test result. The values of the benchmark and v2 structure are close, however. The data from the test samples reveal a difference in concrete strength between printing sessions.

*This statement applies to standard concrete structures.

Average values	Compression		Flexure		Time
	kN	Mpa	kN	Mpa	Days
630x100	74,16	46,34	2,07	4,86	20
630x200v1	71,41	44,57	1,85	4,35	17
630x200v2.1	80,49	50,30	3,18	7,45	11
630x200v2.2	58,96	36,85	2,40	5,62	10
B.2	74,82	46,76	3,10	7,25	17

Table 8 – Results of test samples

Should the difference in flexural capacity be incorporated into the failure load, the results would differ. Accordingly to the formula $\sigma=F/A$, an increase in flexural strength(σ) results in an increase in force(F) if area(A) is a fixed value. The difference in flexural capacity between the average of v.2 and v.1 is a factor $(7,45+5,62)/2 / 4,35 = 1,5$. Multiplying the failure load of v.1 with the difference in flexural capacity results in an estimated failure load of $1,5 \times 7,483 = 11,22\text{kN}$.

The difference in displacement and deflection between all the structures is noticeable. At first, the benchmark results are way higher for defl/disp than the first printed structure, 630x200 v1. This suggests that the structure isn't close to representing the benchmark beam in terms of stiffness. Printed structure v1 doesn't behave like a solid structure but as individual segments with a certain spring value for the joints. The results for defl/kg, disp/kg and kN/kg of the v1 structure are incompatible with comparing the b.2 and v.2 structures due to the difference in material strength. The structure failed at a lower force due to the lower material properties. Because the weight is a constant factor and isn't affected by the material properties, the comparisons between the two structures can't be drawn.

The improved version, 630x200 v2, generates a higher percentage on the defl/disp. Displacement and deflection values are less far apart, indicating the structure behaves more like one solid object. The improved printing route avoids most parallel gaps and incomplete joints. This results in a closer representation of the optimised structure, thereby mimicking the values of the benchmark beam (in terms of stiffness).

The elongation of v2 is noticeably lower than the v1 and benchmark (0,024mm compared to 0,034mm). A possible reason for this low value is the failure mechanism of the v2 printed structure. The expected failure mechanism is a crack in the middle due to the tensile forces in the lower part of the structure, as happened with v1. The v2 printed structure didn't crack in the middle as expected. Because the crack appeared outside the measured elongation, the total elongation (at the crack) is unknown. The measured elongation wasn't fully extended to its maximum potential, resulting in a lower elongation. For this reason, it is incorrect to use the 'stiffness score' for v2 printed structures. The 'stiffness score' is only valid when the crack appears within the measured area.

5 out of 6 v2 printed structures failed similarly, as shown in figure 2, all with a low elongation value. Only the v2 printed structure that failed in the middle showed a higher elongation (0,033mm) and force (14,63kN) than average. The result from this structure (that failed as expected) indicates the potential strength of the structure should there be no execution flaws.



Figure 43 – Expected failure (630x200v.1)



Figure 44- Unexpected failure (630x200v.2)

The reason for the different failure mechanisms compared to the v1 printed structure and expected failure can have different (or a combination) reasons:

- Between v1 and v2, a different approach is used to establish the print route. The location where the v2 printed structures failed is where two separate print paths join (weak spot). The v1 printed structure has a continuous print path at the same location.
- The structure is optimised in stiffness by the TO-script. Because the structure is statically indeterminate internally, the overall stiffness affects the failure load. The suggested improvement for the structure to behave as on solid object has increased the overall stiffness

and, thereby, the maximum load capacity(creating a compression arch). The location where the v2 printed structure failed is the same location where compression- and tensile stresses meet. An increased load combined with a local stress transition can result in local failure.

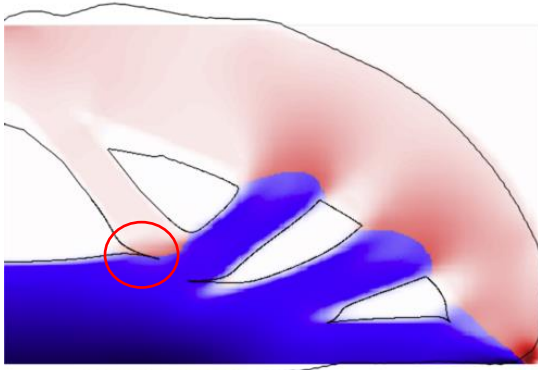


Figure 45 – Stresses TO + outline



Figure 46 – prescribed surface TO

Figure 46 shows a combination of the stress result(red and blue) from the TO script and the outlines of the printed structure(black). Figure 4 shows the prescribed surface from the TO output. The marked location shows the difference in the prescribed surface and executed printing route, at which the printed structure failed.

The beginning of this research started off with topology optimisation of a benchmark beam. This optimisation tool used the variables inserted into the script to generate a structure optimised in stiffness. The data show a 0,004 defl/kg value for the benchmark vs 0,031 (v1) and 0,064 (v2). This suggests that the v1 printed structure outclassed the benchmark with 25% capacity. Unfortunately, the results also show a significantly lower failure load. Because the structure didn't reach around the same failure load as the benchmark of v2 structure, the deflection remained small, affecting the overall defl/kg ratio. Therefore the defl/kg ratio of the v1 structure is excluded from the comparison.

Optimised structure v2 had a score of 0,064 defl/kg. This is a difference of 50% compared to the defl/kg ratio of the benchmark beam. This large difference in defl/kg ratio shows that the optimised beam is not in resemble with the optimised output from the topology optimisation. This difference in deflection is validated via software analysis in chapter 6.1.4.2.

6.1.2.2. Statements

Comparing the different structures with each other gives insight into the behaviour of the structure, structural capacity and the effect of the imposed improvements during design and execution. Comparing the results of the benchmark b.2 solid beams and the optimised 630x200 printed structure v1 and v2 implements the following statements:

1. The optimised structures can achieve the same failure load (or even higher) compared to the benchmark beams once the values of the failure loads are adjusted according to the material properties. By achieving the same failure load, the kN/kg ratio of the printed structures excels the ratio of the benchmark beam. This means the optimisation process achieved a higher kN/kg ratio, a positive effect of the optimisation. The v1 and v2 structures are relatively close regarding

kN/kg performance. The imposed improvement in optimisation and execution doesn't greatly (slight difference between v1 and v2) affect the failure load.

2. There is a difference in stiffness between the benchmark, 630x300v1- and 630x300v2 printed structure. The printed structure is optimised in stiffness, mimicking the same stiffness performance as the benchmark beam. Therefore the goal is to perform as close as the benchmark beam in terms of stiffness. Due to the difference in material properties measured with the test samples, only the defl/disp ratio is correct. Defl/kg or disp/kg are irrelevant because the structure couldn't achieve the same failure load and, thereby, the same deflection. The ratio between defl/disp isn't affected by the material strength.
V1 optimised structure scored 0,333 on a scale of 1, which isn't close to the benchmark score of 0,734. Printed structure v2 achieves a 0,610 score on defl/disp. This value comes close to the benchmark performance. The increasement in defl/disp means the imposed improvement does affect the overall stiffness of the structure. The visual observation of the joints (and therefore imposed improvements) are confirmed with the test results.
3. Failure analysis showed an unexpected failure due to shape and execution choices. Corners with a narrow-angle should be avoided at locations where compression- and tensile stresses meet. This can be incorporated in the choice of print path route during the optimisation process.
4. When comparison the defl/kg ratio the printed structure 630x200 v1 is exciled from the comparison due to early failure. The v2 printed structure shows an increase of 50% defl/kg ratio compared to the benchmark. This shows that the printed structure is not as in accordance with the topology optimisation output.

6.1.3. COMPARING PRESCRIBED WEIGHT VS MEASURED WEIGHT

Comparing the printed- and casted structures with each other gives an insight into the structural properties and the development of execution. However, the goal is not to develop a printed structure with the highest properties but to validate the design tools. A comparison between the digitally optimised- and printed structures gives insight into the accuracy of the process.

After the outcome of the topology optimisation, some digital steps are taken before the structure can be printed. Every step can have a negative or positive effect on the performance of the printed structure. Within this chapter, the weight will be reviewed throughout the process.

Before the optimised structure can be printed, two significant steps must be taken. At first, the conversion of the output from the print path script into a 2D CAD file. Secondly, the 2D CAD file is converted into coordinates that direct the robot.

For this comparison, three different methods are used to determine the weight at a certain stage through the process, namely:

1. The topology optimisation output determines the structure's weight. The area(measured) * thickness(50mm) * volumetric weight(2400kg).

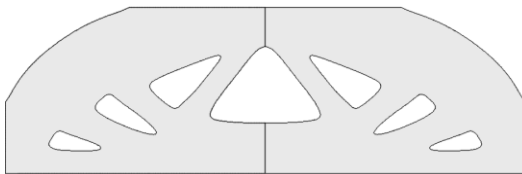


Figure 47 – TO result surface

2. The structure's weight after creating the centre- and outline, generated by the area * thickness(50mm) * volumetric weight(2400kg).

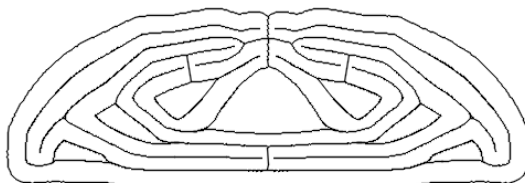


Figure 48- Print path result surface

3. The weight of the printed structure is measured after printing.

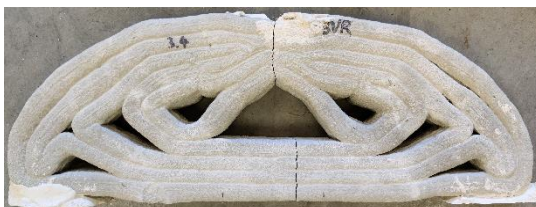


Figure 49 – Printed structure

6.1.3.1. Case study 1

The results in weight and differences between steps give insight into the process and development of the total weight of the structure. Noticeable are the differences between the digital steps. First, the weight is increased, and secondly, decreased, minimalising the overall difference between start and end. Processes that affect the total weight of the structure will be discussed in this chapter.

Weight (kg)	Weight 100% (kg)	Weight TO (kg)	Weight PP (kg)
5,927	5,310	6,240	6,719
6,431	5,145		
5,928	5,335		
6,062	5,456		
6,037	5,433		
5,179	5,179		

Table 9 – Weight 630x100

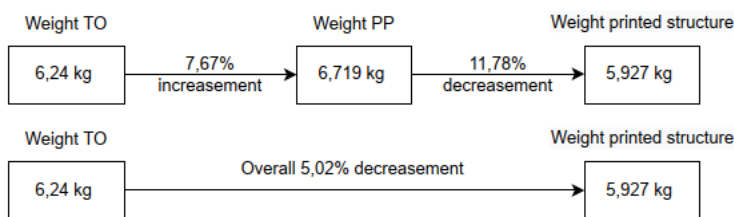


Table 10 – Weight difference 630x100

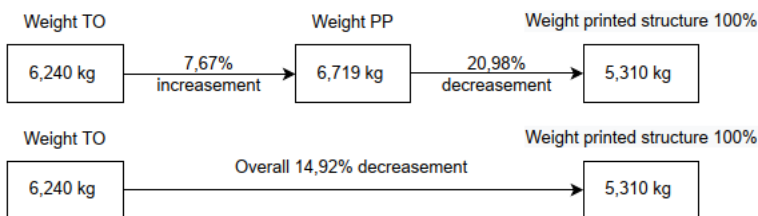


Table 11 - Weight difference 630x100 100% speed

*Printed structures from case 1 are printed with varying(reduced) robot speeds. Lowering the robot's speed increases the total amount of concrete. The figure above shows the weighed structures and the expected weight without a reduced robot speed.

6.1.3.1.1. Toolpath generator

The first reason for the increase in weight comes from using the toolpath generator. This script determines the optimal joint connections combined with a certain amount of print paths, creating one segment. The script can choose a variety of print path widths (between 15-30mm). A negative side effect of a minimum width is the over-dimensioning of the print paths. For example, the print path (purple) of 15mm overlaps the excision (green) prescribed by the TO result. This toolpath's side effect can have a magnifying effect on the total weight of the printed structure.

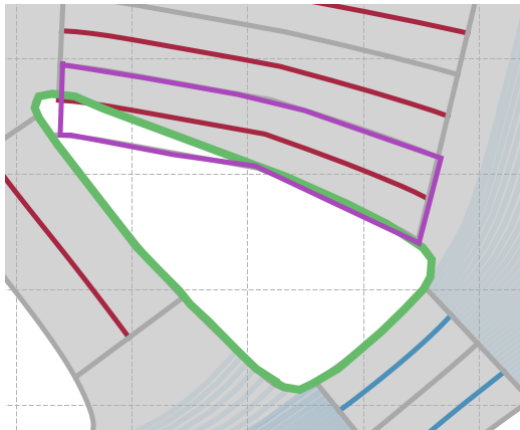


Figure 50 – Outcome toolpath generator

6.1.3.1.2. Voronoi

The second increasement can be explained through the grasshopper component Voronoi, which helps create the outlines from the prescribed centreline. The component expands a circular boundary from a given point until a barrier (another border) exists. By increasing the number of target points for the Voronoi component, squares can be created aligned with the centreline. The edges parallel to the centreline are manually selected and filtered, creating the outlines.

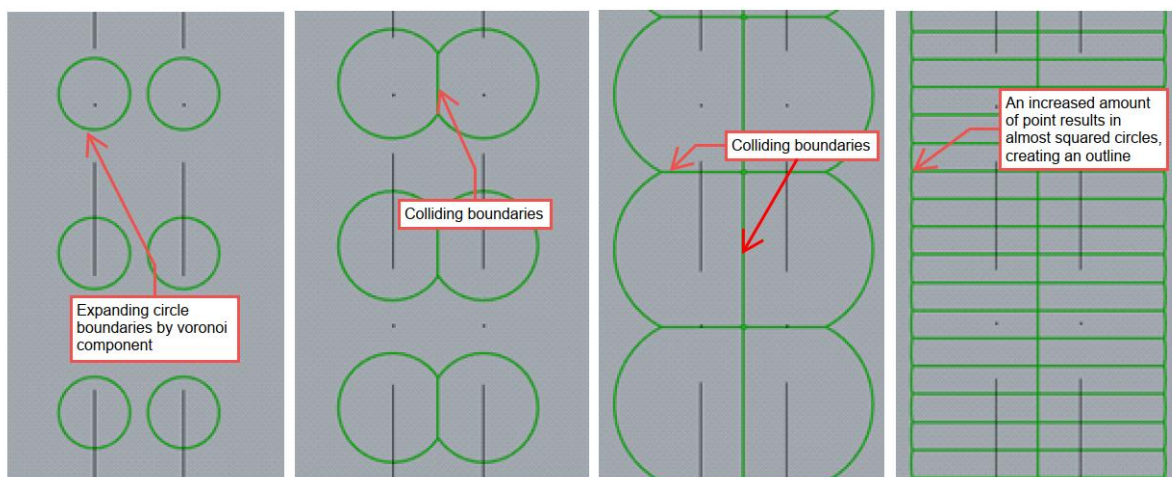


Figure 51 – Voronoi component

Unfortunately, the component continues expanding at locations with no barrier or collision with another circle, creating a wider (on one side) asymmetrical surface than initially wanted. The outlines are created from the given centreline via the Voronoi component. Input for the component is a maximum radius to which the component can expand. With a minimum of 15mm and a maximum of 30mm for the print path

width, the radius needs to be between 7,5mm and 15mm. Problems occur when the radius is set at the lower boundary, as seen in the figure below left. The outline for smaller print paths is correct but incorrect for a print path with a larger width (print paths don't connect to each other).

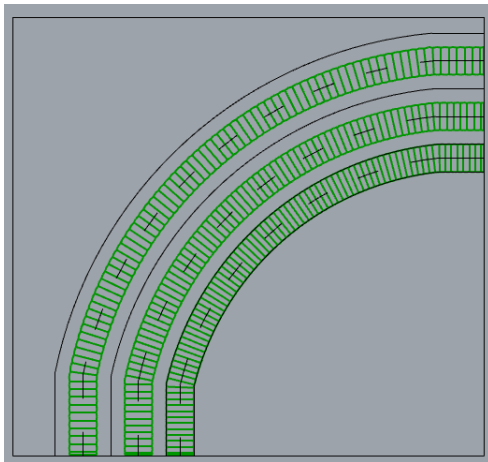


Figure 52

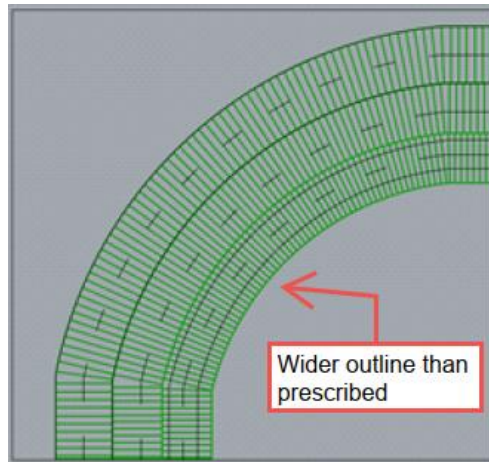


Figure 53

To create print paths attached to each other, the radius for the Voronoi component is increased to the maximum print path with, namely 15mm. A negative side effect is the over-dimensioning of the print paths. If a smaller path is placed at the edge of a concrete section, the component pushes the outline further than the previous software programs intended, as in the figure above. This happens because there is no collision with another boundary. This over-dimensioning of the print paths can be corrected manually. Outlines on the outside of the structure can be trimmed back to the minimum print path width.

This solution is impossible for all situations, as shown in the figure. The green line is the prescribed outline from the TO script. As described in this chapter, the PP script excels at this boundary to obtain the optimal number of print paths. The Voronoi component pushes the outline further (15mm instead of the prescribed 7,5mm) because there is no adjacent boundary. In this case, trimming the outline back toward the prescribed outline from the TO result is impossible due to the minimum print path width. These alternations of the prescribed outline result in a 46% reduction of the opening in the printed structure. The reduction value is specific to this situation.

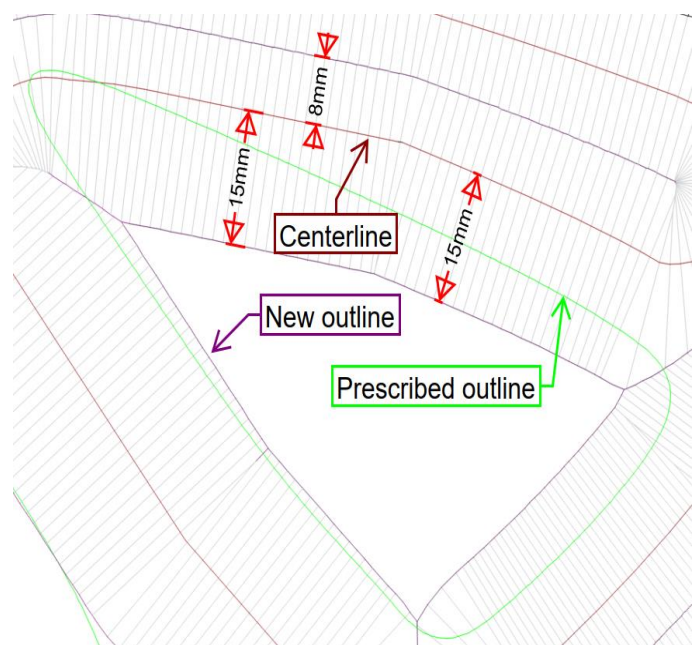


Figure 54 -

The negative side effect of the component Voronoi can partly be prevented by adding a boundary condition to the print path generator. In previous examples, the small print path was placed on the outside of a cross-section, which resulted in over-dimensioning. By placing print paths with a maximum width on the outside and varying lanes on the inside, the component Voronoi stops at the prescribed outline, as shown in the picture below. This solution is not possible in all situations.

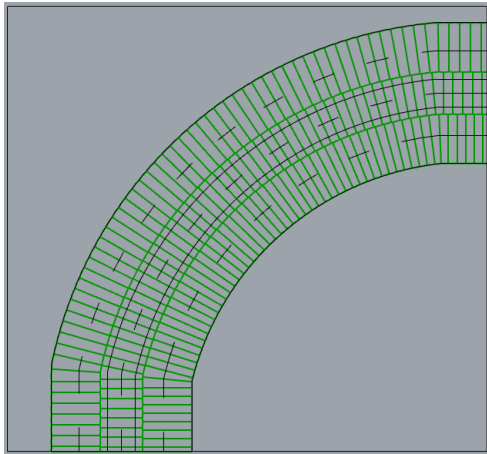


Figure 55 – optional solution

6.1.3.2. Case study 2

The difference in weight fluctuates a lot between the 2D input in the grasshopper and the 3D printed outcome after the 2nd major step. Changes in printing routes and execution are made to create a 3D beam representing the 2D version as closely as possible. Overlapping layers, adaptation in centrelines, and re-routing the print path have made a printed structure representing the TO output very close(-4,53%).

Weight (kg)	Weight 100% (kg)	Weight TO (kg)	Weight PP (kg)
11,049	10,118	11,996	12,975
11,423	10,281		
11,367	10,230		
10,457	10,457		
11,368	10,231		
10,352	9,317		
11,327	10,194		

Table 12 – Weight 630x200v.1

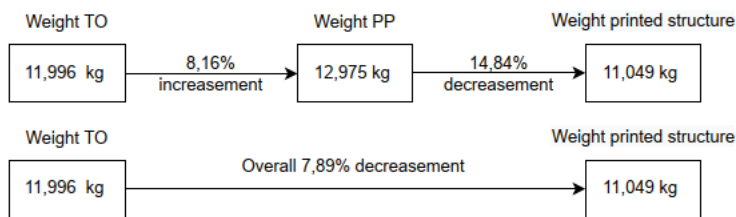


Table 13 - Weight difference 630x200v.1

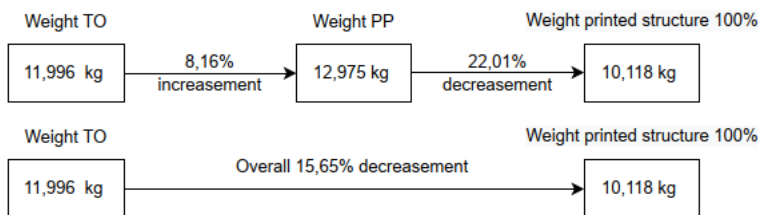


Table 14 - Weight difference 630x200v.1 100% speed

Weight (kg)	Weight 100% (kg)	Weight TO (kg)	Weight PP (kg)
11,452	11,452	11,996	12,975
11,271	11,271		
11,537	11,537		
11,584	11,584		
11,600	11,600		
11,398	11,398		
11,322	11,322		

Table 15 - Weight 630x200v.2

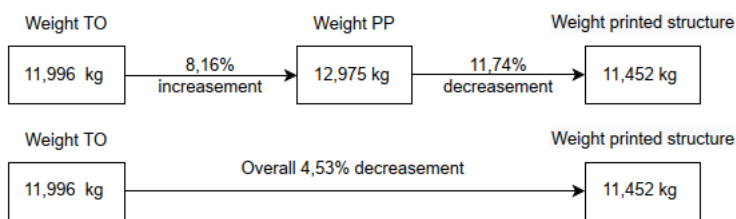


Table 16 - Weight difference 630x200v.2

The process within the grasshopper creates a weight reduction compared to the area created by the outlines. The first reason for this deviation is the possibility of air plugs within the concrete hose. These short interruptions in concrete flow can appear when the concrete clumps up in the funnel, creating a cavity at the pump’s screw. This effect can be countered by pushing the concrete downwards with a stick through the funnel. This has to be done manually, which leaves room for errors in the process.

Some gaps between print paths or joints are still present. This affects the total weight of the printed structure. The improvements in execution have a positive effect. Printed structures from case 3 look more solid than those from case 2. The numbers also confirm that. Looking at case 2.2, there are still some gaps. Further improvements in execution and optimisation can reduce the difference in weight more, but only for a small amount. The increase in weight between the TO result and Autocad is hard to tackle due to the use of the toolpath script. This negative effect can be reduced by reducing the range for width per print path. Increasing the structure's size also benefits the toolpath script's calculation capacity.

6.1.4. EXPERIMENTAL RESULTS VS NUMERICAL RESULTS

The last comparison made for this research is between the results of the printed structure 630x200 v.2 and the software calculation. The TO script prescribed a geometry optimised according to the imputed boundaries, material properties and point load. In addition to the printing of the structure, the prescribed geometry is tested within Grasshopper via the Karamba tool. The virtual and printed test results are put side by side to review the difference between virtual- and reality.

The previous comparisons were drawn to give an insight into the improvement in execution and relation to the benchmark beams. This comparison purely focuses on the difference in results between virtual- and reality.

Two different geometries are calculated within Grasshopper. The first geometry is a simple beam, the 630x200 benchmark. In previous chapters, the deviation between optimised and printed structures are described. These deviations affect the structural behaviour. To give insight into the effect of these deviations, a single beam is recalculated via Karamba. Due to the simplicity of the shape, it is easy to set up the calculation within Grasshopper and check if the results correspond. Once the script works according to plan, more complex shapes, such as the optimised beam, can be inserted. The second geometry tested is the toolpath generator's direct output. These results should be the supposed values after all the optimisations.



Figure 56 – Karamba benchmark structure



Figure 57 – Karamba optimised structure

6.1.4.1. Comparison benchmark

The first geometry for comparison is the benchmark 630x200 beam. This structure is schematised as a simply supported beam, vertically supported left and right and horizontally supported on the right side.

Two data points are used for this comparison: The maximum displacement (measured at the top in the middle of the structure) and maximum deflection (measured at the bottom). The average experimental data values will be compared with the software values. To obtain the software values, the average failure load from the 3PBT is used as input for the Karamba calculation to determine the displacement and deflection.

	Experiment data			Software data		
	Displacement (mm)	Deflection (mm)	defl / disp	Displacement (mm)	Deflection (mm)	defl / disp
630x200 benchmark	1,372	0,995	72,5%	1,007	0,795	78,9%

Table 17 – Deformation benchmark

The experimental- and software data values show a minimum deviation between the deflection and a slight deviation in displacement. The difference in defl/disp is relatively small. When taking a closer look at the experimental defl/disp values, it is visible that the average value is affected by a sample that differs a lot (83%, 55% and 82,1%). Should the 55% be considered outside the acceptable margin, the difference between the experimental- and software data will be; $(83+82,1)/2-78,9\%=3,65\%$. With this small deviation in values, it can be stated that the Karamba calculation resembles the experimental test. The difference in result can be written off by the difference in material (C30/35 instead of 3DCP mortar), the hardening time (17 days instead of 28 days), and possible errors in execution

Both the experimental and software data show a difference between displacement and deflection. At first, this suggests that the structure doesn't behave stiff enough and gets compressed. The structure consists of pure concrete, which gives it a strong but brittle behaviour. There is no ductile behaviour in the structure, which excludes rotational movements of the joint that can cause the deformation difference.

Normally, 3-point bending test results in pure bending, with compression in the upper part and tension in the lower part of the structure. The horizontal forces result in horizontal deformations, creating a positive elongation in the lower part of the structure. The opposite happens in the compression part, squeezing the material together creating a shorter length.

The 630x200 structure is on the verge of being considered a deep beam (length < height * 3). Instead of pure bending, forces are directed directly to the supports, creating two diagonal compression zones with one horizontal tension area. The diagonal compression zones result in deformation in 2 different directions, namely horizontal but also vertical. This distribution of stresses directly to the support creates an internal deformation without bending (and creating a deflection) the whole structure.

This theory is tested via a Karamba simulation. The same benchmark beam is enlarged horizontally, creating a situation with pure bending. The data shows a reduction in the difference between deflection and displacement.

	Displacement (mm)	Deflection (mm)	defl / disp
630 x 200 benchmark	1,0070	0,7950	78,9%
1000 x 200 benchmark	1,1900	1,1700	98,3%

Table 18 – difference defl/disp simpel beam vs deep beam

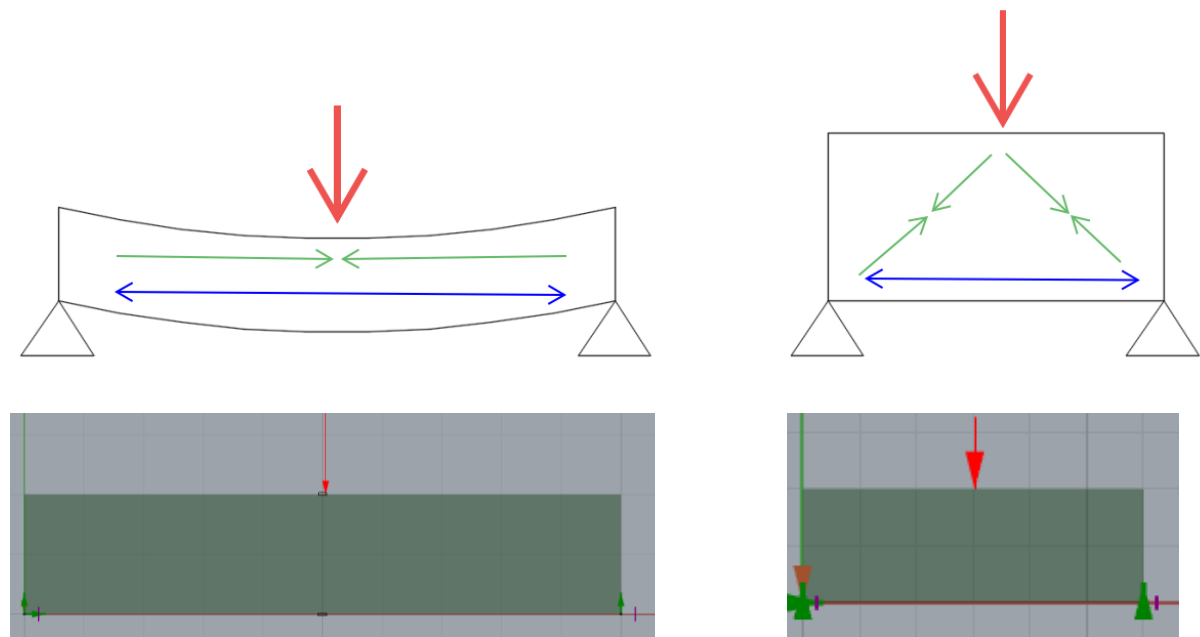


Figure 58 simpel beam vs deep beam

6.1.4.2. Comparison optimised structure

The displacement and deflection are calculated for v.1 and v.2 printed structures. For each case, the average failure load is applied (v.1= 7,483kN v.2=13,087kN).

	Experiment data			Software data		
	Displacement (mm)	Deflection (mm)	defl / disp	Displacement (mm)	Deflection (mm)	defl / disp
630x200 v1	1,474	0,492	33,3%	0,611	0,402	65,8%
630x200 v2	2,222	1,345	60,5%	1,064	0,699	65,7%

Table 19 – Deformation Case study 2

The results show several noticeable values:

- The overall difference in displacement is large. The experimental displacement for v.1 is 2.5x larger, and for v.2 2x larger.
- The v.2 deflection has the same magnitude factor between the experimental- and software data, namely 2x larger.
- The v.1 deflection doesn't have the same magnitude factor between the experimental- and software data. Here the difference is only 1.22x. This difference is also visible between the defl/disp values.

The improvement made to improve the structure's stiffness are visible in the result. Where the v.1 printed structure failed to behave like the TO-output, the overall stiffness of the v.2 printed structure is relatively close regarding the defl/disp ratio.

The large difference in overall displacement is remarkable. These large differences only occur when comparing the optimised beam with the digital results. The benchmark beams don't show large deviations between experimental- and software results. The supports are the only difference in testing between the benchmark and printed structures. Due to the irregular surface of the printed structure and the height difference between the structure's middle and end (+5mm), gyps supports are casted to create a flat surface. Benchmark beams already have a flat surface, so no gyps are applied. It is plausible that the gyps support allowed some vertical deformation, resulting in an overall vertical translation of the tested structure.

7. CONCLUSION AND RECOMMENDATION

In this final chapter, a conclusion will be attached to the knowledge obtained throughout the execution and analysis of this research. Besides the conclusion, a recommendation is drafted as a setup for further research in applying design tools for 3DPC.

7.1. Conclusion

This research is set up to optimise, execute and test a structure and see whether the input and outcome comply with each other, a validation process. The validation is conducted between virtual reality (software calculations) and reality (tested structures). Besides the validation between the virtual- and real world, a comparison is drawn between printed- and casted structures (benchmark) to visualise the effect of optimisation. During this process, the hurdle of printing a 3D solid structure with polylines (varying in volume) adds an extra dimension to the validation.

7.1. PRINTED STRUCTURE VS BENCHMARK

The following conclusions can be drawn from the comparison and discussion regarding the printed structure vs the benchmark beam:

- The optimised structure can achieve a higher kN/kg ratio than the benchmark beam.
- The printing route and execution choices do not affect the kN/kg ratio but alter the structure's stiffness. Insufficient joint and non-consecutive print lanes have a negative effect on the overall stiffness of the printed structure.
- The optimised structure is optimised in stiffness but can't achieve the same stiffness as the benchmark beam, which served as input for the optimisation.

7.2. REALITY VS VIRTUAL REALITY

The following conclusions can be drawn from the comparison and discussion regarding reality vs virtual reality:

- Between the TO results and the measured weight, a decrease of 4,53% results in a relatively close result. In between phases, the amount of weight increases and decreases. The increasement in weight between the TO and PP step can be explained by the overlapping layers due to the minimal and maximal print width. The weight between PP and printed structure should remain the same, but this is not the case. This means there is room for improvement in this step, resulting in a printed structure heavier than the prescribed weight from the TO.
- There is a difference in deformation between the experimental and numerical results. This indicates the stiffness of the printed result doesn't fully resemble the optimised beam.

7.3. VALIDATION

With all the data assessed, analysed and discussed, an overall conclusion can be formulated to answer the research question, which is:

“ Can it be stated that the design models are valid in resemblance with reality?”

The answer to this research question can be divided into 3 different aspects; force/weight ratio, stiffness and overall weight:

- Force/weight ratio, the results (adjusted with the test sample results) show a kN/kg ratio higher than the benchmark beam. This validates the goal of optimisation, which is to maximise the system’s performance.
- Stiffness, there is a difference in deformation between the tested and virtual structures. This difference can be traced back to execution errors. Incorrect joints, sharp angles and unparallel print paths reduce the cohesiveness of the structure. The imposed improvement in execution shows a stiffness that is getting more similar to the virtual structure but still differs too much to say the printed structure resembles the virtual reality.
- Weight, the overall weight does resemble the design model. Slight deviations can be traced back to using the print path tool, robot script and robot control. The robot script leaves room for further adjustments to optimise the structure, but there will always be a difference between the structure’s virtual- and actual weight due to the minimum and maximum print width.

The overall conclusion of this research is that the main challenge in the step between virtual- and actual reality is the execution. Choices in the printing route, limitations in printing width, and external factors like the printing bed, concrete mix, and robot speed all affect the execution, altering the result compared to the digital version. The step from 2D virtual to 3D reality seems relatively small, but minor alterations significantly affect the result.

7.2. Recommendation

During optimisation, execution and testing, several obstacles had to be overcome to create a structure that resembles the TO result. A list of attention points is created to improve the outcome of the printed structure:

1. To avoid gaps at joints, adjacent print paths should overlap, as described in chapter 4.2.2.5.
2. Enough hardening time between printing layers is necessary to ensure the buildability of the structure. If the layers are stacked too fast, the lower layers of the structure will collapse and be spread out, as described in chapter 4.3.2.3.
3. Adjacent print paths with sharp angles should be avoided in stress transition zones, as described in chapter 6.1.2.2.

Manual adjustment and digital implication during the process of transforming a 2D surface into a 3D structure create a difference in result compared to the TO output. To prevent over-dimensioning of print paths, described in chapter 6.1.3.1.2, the PP script should incorporate the following rule: If a structural rib has 3 or more printing lanes, the outer lanes should be maximised, and smaller lanes must be placed in the middle. This adjustment prevents over-dimensioning with the Voronoi tool in Grasshopper.

In chapter 6.1.3. the transition from TO result to printed structure in terms of weight is reviewed. The second step, from PP to printed structure, showed such a decrease that the overall weight of the printed structure ended up lower than the prescribed weight from the TO. Further finetuning of the grasshopper script, better incorporation of the robot speed and rotational delays, and guaranteeing a constant concrete flow should all decrease the difference between the PP phase and the printed structure's weight.

Once the process of transforming a 2D surface into a 3D structure is mastered and a certain level of resemblance is achieved, further research of different shapes lies open. The optimisation possibilities for the TO script were somewhat limited due to the boundary conditions (simply supported beam). Broadening these boundary conditions will generate more challenging but exciting structures where the TO script is used entirely to its potential.

Due to the lack of data and material properties, reinforced concrete is left out of this research. This limits the TO script in optimising a structure (due to the low tensile strength of concrete). Incorporating reinforcement in optimisation would expand the possibilities in optimisation even further. This can only be incorporated once the material properties are known for sure.

REFERENCES

- [1] C. Lynch, "The construction industry is getting greener why how and whats changing," 25 August 2021. [Online]. Available: <https://www.forbes.com/sites/sap/2021/08/25/the-construction-industry-is-getting-greener-why-how-and-whats-changing/?sh=16fe2f7052bc>.
- [2] J. W. S. D. X. Y. B. H. J. Zhang, "A review of the current progress and application of 3D printed concrete," Composites part A 125, Dalian Univeristy of Technology, 2019.
- [3] "Shape optimization," 6 July 2022. [Online]. Available: https://en.wikipedia.org/wiki/Shape_optimization.
- [4] "Topology optimization," 31 August 2022. [Online]. Available: https://en.wikipedia.org/wiki/Topology_optimization.
- [5] J. Versteeg, "An integrated approach for topology optimization and print path generation of cable-reinforced 3D printed concrete structures," Eindhoven University of Technology, 2020.
- [6] "Robot Studio," ABB, 2004. [Online]. Available: <https://forums.robotstudio.com/discussion/74/differences-movejoint-moveline>. [Accessed December 2022].
- [7] Wikipedia, "Linear variable differential transformer," 27 October 2022. [Online]. Available: https://en.wikipedia.org/wiki/Linear_variable_differential_transformer. [Accessed 2022].
- [8] Z. Y. A. E. R. J. T. A. S. Freek P. Bos, "Experimental exploration of metal cable as reinforcement in 3D printed concrete," Materials MDPI, Deventer, 2017.
- [9] F. B. T. S. R.J.M. Wolfs, "Hardened properties of 3D printed concrete: The influence of process parameters on interlayer adhesion," Cement and Concrete Research 119, Eindhoven University of Technology, 2019.
- [10] MAI international, "MAI," MAI international, 2020. [Online]. Available: <https://www.mai.at/plastering-systems/delivery-pumps/mair2pump-pictor/>. [Accessed 2022].

| APPENDIX